AGU100 ADVANCING EARTH AND SPACE SCIENCE

JGR Solid Earth

Key Points:
- First platinum-group element (PGE) and Re-Os isotope results for peridotites of Paleo-Tethys ophiolites in southwest China
- Ancient refractory mantle domains are preserved in the mantle peridotites
- Plagioclase lherzolites were converted from the ancient refractory domains by refertilization much earlier than the seafloor spreading

Supporting Information:
- Supporting Information S1

Correspondence to:
H. Zhong,
zhonghong@vip.gyig.ac.cn

Ancient Refertilization Process Preserved in the Plagioclase Peridotites: An Example From the Shuanggou Ophiolite, Southwest China

Wen-Jun Hu[1,2], Hong Zhong[1,3] (iD), Zhu-Yin Chu[4] (iD), Wei-Guang Zhu[1], Zhong-Jie Bai[1], and Chang Zhang[4]

[1]State Key Laboratory of Ore Deposit Geochemistry, Institute of Geochemistry, Chinese Academy of Sciences, Guiyang, China, [2]Department of Earth Sciences, University of Hong Kong, Hong Kong, China, [3]College of Earth and Planetary Sciences, University of Chinese Academy of Sciences, Beijing, China, [4]State Key Laboratory of Lithospheric Evolution, Institute of Geology and Geophysics, Chinese Academy of Sciences, Beijing, China

Abstract Petrology, geochemistry, platinum group elements (PGEs: Os, Ir, Ru, Rh, Pt, and Pd), and Re-Os isotope data of harzburgites and plagioclase lherzolites from the Shuanggou ophiolite (southwest China) are presented in this study, in order to determine whether ancient refertilization process can be preserved in ophiolitic plagioclase peridotites. The harzburgites in the Shuanggou ophiolite are divided into two groups: (1) the Group-1 harzburgites have $^{187}Os/^{188}Os$ ratios (0.12297–0.12727) and PGE abundances similar to those of oceanic peridotites, thereby representing the convecting upper mantle; (2) the Group-2 harzburgites have extremely low $^{187}Os/^{188}Os$ ratios (0.11307–0.11651) with considerable fractionation in iridium group PGEs (Os, Ir, and Ru), indicative of an ancient refractory mantle in the oceanic lithosphere. The plagioclase lherzolites were formed by melt impregnation of the Group-2 harzburgites, according to the PGE compositions and the petrographic features. However, the large Os isotope difference between the lherzolites ($^{187}Os/^{188}Os$: 0.12470–0.12666) and the Group-2 harzburgites indicates that the refertilization process took place much earlier than the exhumation of the mantle at 0.4 Ga. In addition, clinopyroxene composition suggests that the percolating melt is different from the Shuanggou diabases and typical mid-ocean ridge basalts. This study therefore demonstrates that some plagioclase lherzolites possibly were not related to mantle exhumation beneath the spreading center but formed by much older melt impregnation processes in the mantle instead.

1. Introduction

Mantle refertilization refers to the process whereby refractory mantle residues (e.g., harzburgites) transform into fertile mantle rocks (e.g., lherzolites and pyroxenites) by addition of melts (Elthon, 1992; Le Roux et al., 2007; Müntener et al., 2004, 2010; Rampone et al., 2009; Rudnick & Walker, 2009). This process critically influences the mantle-crust system, by changing compositions and lithologies of the upper mantle and consequently affecting the mantle-derived magma (Foley, 2008; Hirschmann & Stolper, 1996; Kogiso et al., 2004; Le Roux et al., 2007; Lee et al., 2011; Yaxley, 2000).

Plagioclase peridotites are widely distributed in passive continental margins, slow-spreading ridges, and ophiolitic mantle sections (Dick, 1989; Müntener et al., 2004, 2010; Nicolas & Dupuy, 1984; Piccardo et al., 2004; Rampone et al., 1994, 1997, 2009; Saal et al., 2001). Although some plagioclase peridotites might be formed by subsolidus recrystallization of spinel peridotites under plagioclase facies conditions (e.g., Hamlyn & Bonatti, 1980), most of them are generated by melt impregnation into depleted peridotites (e.g., Müntener et al., 2004, 2010). Therefore, plagioclase peridotites have been widely used in studies of the refertilization process. However, the formation time of the plagioclase peridotites is largely uncertain, because direct dating is extremely difficult at present. In most cases, formation of plagioclase peridotites is expected to be a natural consequence of interaction between extending lithosphere and upwelling asthenospheric melts during continent breakup and seafloor spreading. For example, several plagioclase lherzolites in Eastern Central Alps in eastern Switzerland and northern Italy have been proposed as "lithospheric sponges" whereby melt stagnates in the mantle during the ocean-continent transition, based on evidence
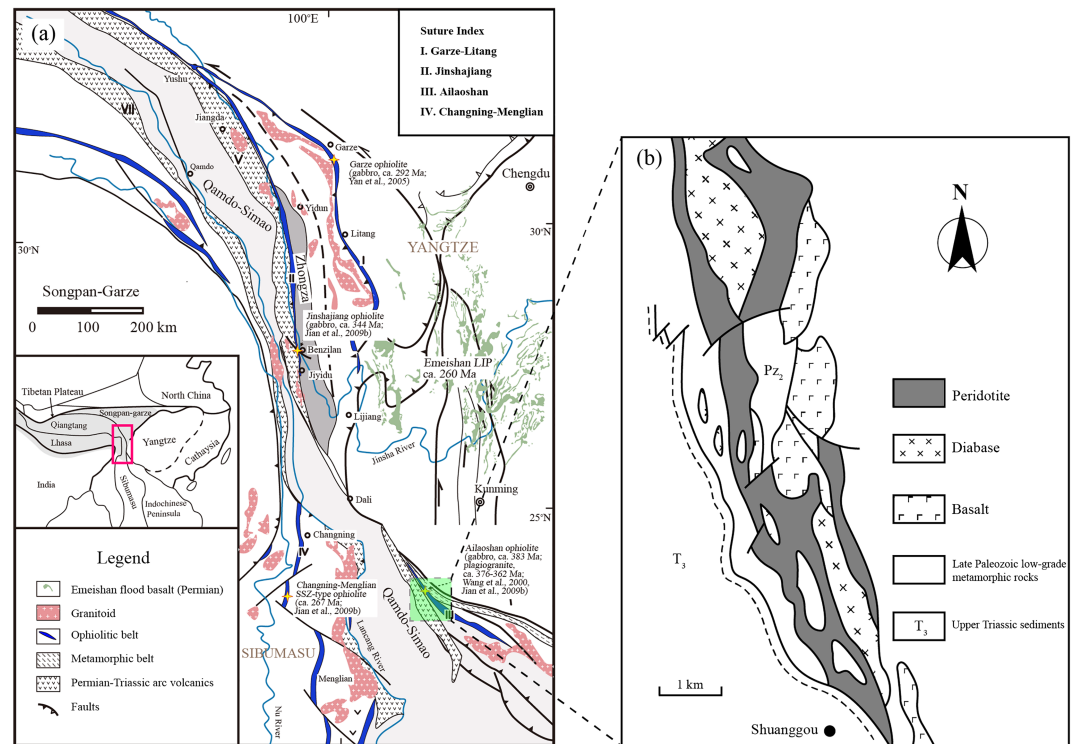
Figure 1. (a) Index map of the major Paleo-Tethys suture zones (ophiolitic belts) and tectonic units in the Sanjiang area, southwest China (after Zi et al., 2012) and (b) geological map of the Shuanggou ophiolite (after Zhang et al., 1995)

from clinopyroxenes in the plagioclase lherzolites, which show Nd isotope compositions similar to the associated oceanic crust (Müntener et al., 2004, 2010).

In contrast, recent studies on layered pyroxenites embedded in mantle peridotites highlight the fact that fertile mantle rocks in the shallow mantle could be generated by episodic or continuous refertilization process through the mantle history, not just simply before or during the exhumation of the mantle (Borghini et al., 2013; Le Roux et al., 2016; Le Roux & Liang, 2019). In the light of these studies, we chose plagioclase lherzolites and associated harzburgites from the Shuanggou ophiolite to detect whether ancient refertilization process could be recorded by some ophiolitic plagioclase peridotites. The Shuanggou ophiolite is the best preserved part of the Ailaoshan ophiolitic belt which formed by closure of a branch ocean of the Paleo-Tethys (Figure 1) (Mo et al., 1998; Zhong, 1998). The mantle sequence of the ophiolite is dominated by well-exposed plagioclase lherzolites with a smaller portion of harzburgites (Jian et al., 2009a, 2009b; Zhang et al., 1995; Zhong, 1998). Previous studies on the mantle sequence indicated a role of melt impregnation in the formation of the lherzolites (Mo et al., 1998; Zhang et al., 1995; Zhou et al., 1995). Specially, mafic minerals (e.g., clinopyroxenes) in the lherzolites have isotope compositions ($\varepsilon_{Nd}(t) = -1$ to $+3$) different from that of diabases in the crustal sequence ($\varepsilon_{Nd}(t) = +9.7$ to $+11.6$) (Zhou et al., 1995; Hu et al., 2014), which is not common in studies on plagioclase peridotites in the magma-poor rifted margins (e.g., Müntener et al., 2004).

The main methods in this study are the platinum group elements (PGEs: Os, Ir, Ru, Rh, Pt, and Pd) and the rhenium-osmium isotope system ($^{187}Re \rightarrow {}^{187}Os + \beta^-$; $\lambda = 1.67 \times 10^{-11}$ yr^{-1}; Smoliar et al., 1996) in peridotites. PGEs are highly siderophile elements (HSE) with strong affinities for metallic phases and sulfides and therefore could provide unique details about processes in the upper mantle, compared with the commonly used lithophile elements (Lorand et al., 2008). The Re-Os isotope system has shown great potential in studies of mantle peridotites (Carlson et al., 2008; O'Driscoll et al., 2012, 2015; Rampone & Hofmann, 2012; Rudnick & Walker, 2009). Because Re (incompatible) and Os (compatible) behave differently during melting (e.g., Fonseca et al., 2011; Mallmann & O'Neill, 2007), the

melting process can create significant Re-Os fractionation between residues and melts, which, through time, will lead to distinct Os isotope compositions between the two members. Therefore, the Re-Os isotope system is efficient in tracking mantle-melt interactions and distinguishing different mantle domains (Ackerman et al., 2009, 2013; Carlson et al., 2008; Harvey et al., 2010, 2011; Luguet et al., 2007; Marchesi et al., 2014; O'Driscoll et al., 2012, 2015; Rudnick & Walker, 2009).

Because of the different properties of Re and Os in the mantle processes, the Re-Os isotope system can be used to date mantle processes (Rudnick & Walker, 2009; Walker et al., 1989). On the one hand, different model ages of Os isotopes have been established in order to constrain the depletion age of the mantle (Rudnick & Walker, 2009). For example, the rhenium-depletion ages (T_{RD}) is the model age determined by the intersection between the measured $^{187}Os/^{188}Os$ ratios of the bulk rocks with a mantle evolution curve. According to T_{RD} ages, a group of ancient refractory peridotites (~2 Ga) has been identified in the Gakkel ridge, indicating that refractory domains in the lithosphere can remain undisturbed by mantle convection for long periods of time (Liu, Snow, et al., 2008). On the other hand, refertilization would shift the Re/Os ratios of refractory mantle toward higher values (Marchesi et al., 2014; Rudnick & Walker, 2009). With time, the fertile mantle domains will evolve to more radiogenic Os isotope compositions than their protolith (Saal et al., 2001; Sun et al., 2017). Therefore, Os isotope could be used to identify ancient refertilized mantle domains. For example, in Obnazhennaya (Siberian craton), lherzolite xenoliths exhibit higher $^{187}Os/^{188}Os$ ratios than other types of mantle xenoliths. These lherzolites have been proposed to represent refertilized ancient mantle rather than juvenile mantle accreted beneath the craton (Sun et al., 2017).

Here we combine PGE geochemistry and Re-Os isotopes to investigate the mantle peridotites in the Shuanggou ophiolite. Our aims are (1) to clarify genesis and relationships of different types of mantle peridotites (e.g., harzburgites and lherzolites), (2) to estimate their formation ages, and (3) to obtain general implications of refertilization in shallow mantle.

2. Geological Setting and Sample Description

The Ailaoshan ophiolitic belt in the eastern part of the Sanjiang orogen marks an important branch ocean of the Paleo-Tethys Ocean, that is, the Ailaoshan Ocean, which once separated the Qamdo-Simao Block from the Yangtze Block (Figure 1a) (Deng et al., 2014; Jian et al., 2009a, 2009b; Metcalfe, 1996, 2006; Mo et al., 1998; Wang, Metcalfe, et al., 2000; Zhong, 1998). The metamorphic basement of the Qamdo-Simao block is constituted by the 1,437 ± 17 Ma Damenglong and Chongshan complexes (Wang, Li, et al., 2000; Wang, Metcalfe, et al., 2000; Zhong, 1998). Lower Ordovician metasedimentary rocks that outcropped in the Qamdo-Simao block consist of slates, phyllites, quartzites, and marble, which are lithologically comparable to Lower Ordovician rocks in the Yangtze Block. The Lower Ordovician strata are uncomfortably overlain by the Middle Devonian strata which comprises shallow-marine sediments and basal conglomerates. Shallow-marine sediments are the dominant facies all through the Carboniferous-Triassic period in Qamdo-Simao block, that is, the Carboniferous and the Permian strata comprise paralic clastics with coal interlayers, whereas the Triassic stratum is mainly composed of detritus and carbonates (Bureau of Geology and Mineral Resources of Yunnan Province (BGMRYP), 1990; Metcalfe, 2006). Stratigraphic evidence above implies that the Qamdo-Simao Block rifted from the Yangtze Block since the Middle Devonian, resulting in the opening of the Ailaoshan Ocean (Wang et al., 2006; Wang, Metcalfe, et al., 2000; Zhong, 1998).

The Ailaoshan ophiolitic belt is sandwiched between an eastern high-grade metamorphic belt and a western volcanic belt. The eastern metamorphic belt is made of metasedimentary rocks (e.g., greywacke, chert, and limestone) that are derived from the continental margin of the Yangtze block (Leloup et al., 1995; Searle et al., 2010), while the western volcanic belt comprises Carboniferous-Triassic basaltic-granitic rocks that are formed due to closure of the Ailaoshan ocean (Lai et al., 2014) (Figure 1a). As the best preserved part of the Ailaoshan ophiolitic belt, the Shuanggou ophiolite is constituted by mantle peridotites, gabbros, diabases, and basalts, without layered gabbros and sheeted dykes (Figure 1b) (Mo et al., 1998; Zhong, 1998). Small-size plagiogranites are discovered in some diabases (Jian et al., 2009a, 2009b). The crustal sequence of the ophiolite as represented by the diabases exhibits compositions similar to the normal mid-ocean ridge basalt (N-MORB) (Hu et al., 2014). Jian et al. (2009b) reported Late Devonian ages for a diabase (382.9 ± 3.9

Ma) and a plagiogranite sample (375.9 ± 4.2 Ma). The mantle peridotites, which are intruded by gabbros and diabases, mainly comprise plagioclase lherzolites with a smaller portion of harzburgites. The lithological characteristics of the Shuanggou ophiolite, including the dominance of lherzolite in the mantle section, minor portions of mafic rocks, and absence of sheeted dykes, are analogous to those formed at continental margins and slow spreading ridges (Montanini et al., 2008; Pamić et al., 2002; Schaltegger et al., 2002). Therefore, the Shuanggou ophiolite is accepted as an ophiolite formed at a slow-spreading ridge setting or at continent-ocean transition (Jian et al., 2009a, 2009b; Zhang et al., 1995; Zhong, 1998). Peridotite samples in this study are harzburgites and plagioclase lherzolites, according to the modal variability of clinopyroxene. The samples are variably serpentinized with estimated degrees from 30% to 70%, but the textural features are largely preserved. Most harzburgites in the Shuanggou ophiolite show porphyroclastic textures and are composed of olivine, orthopyroxene, and chrome spinel (Figure 2a). Two harzburgite samples (SG1103 and SG1107) in this study show melt impregnation features as is evidenced by the presence of plagioclase (Figure 2b). In the lherzolites, the porphyroclastic assemblage has partially been replaced, or cut, by a second generation of veins or pockets composed of pyroxene and plagioclase (Figures 2c–2f). The plagioclases have been subsequently replaced by hydrogrossular during hydrothermal alteration, according to the reaction (Coleman, 1967): $CaAl_2Si_2O_8$ (anorthite) $+ 2Ca^{2+} + 3H_2O + 0.5SiO_2 \rightarrow Ca_3Al_2Si_{2.5}O_{10}(OH)_2$ (hydrogrossular) $+ 4H^+$.

3. Analytical Method

Whole-rock major elements were analyzed using X-ray fluorescence at the Australian Laboratory Services P/L. Trace element compositions were measured using an inductively coupled plasma mass spectrometry (ICP-MS) at the State Key Laboratory of Ore Deposit Geochemistry, Chinese Academy of Sciences (SKLODG), following the procedure of Qi et al. (2000). The relative standard deviation for both the major and trace element analysis is <5%.

In situ analysis of clinopyroxenes in the lherzolites was analyzed by an Agilent 7900× ICP-MS (laser ablation-ICP-MS) coupled with Coherent GeoLasPro 193-nm Laser Ablation system at the SKLODG following the experimental conditions and procedures from Liu, Hu, et al. (2008). Before introduction into the ICP, the carrier gas (helium) and the make-up gas (argon) were mixed via a Y-connector. The gas flow was added by nitrogen for the purpose of improving the detection limit and precision (Hu et al., 2008). A beam size of 60 μm was adopted for the ablation and each analysis comprised 20–30 s of background acquisition (gas blank) followed by 40 s of data acquisition. NIST610 was analyzed before and after every 10 analyses of the samples to correct for the effect of sensitivity and mass discrimination from time-dependent drift. Calibration was carried out using multiple reference materials (NIST610, BCR-2G, BIR-1G, BHVO-2G, and GSE-1G) without applying internal standardization (Liu, Hu, et al., 2008). Two reference materials (ML3B-G and BCR-2G) were analyzed in this study as unknown samples to monitor the data quality. Off-line selection and integration of background and analytical signals, time-drift correction, and quantitative calibration were performed by the ICPMSDataCal software after Liu, Hu, et al. (2008). Repeated analytical results of international glass standard ML3B-G and BCR-2G are in accordance with their reference values within ±10% with precision better than 10% (relative standard deviation).

Whole-rock PGE concentrations were performed following Qi et al. (2011). Eight grams of powder was mixed with the isotope spike (^{101}Ru, ^{193}Ir, ^{105}Pd, and ^{194}Pt) in a 120 ml Polytetrafluoroethylene (PTFE) beaker (Qi et al., 2004; Qi et al., 2011). Water and HF were added and evaporated to remove the silicates. After addition of HF and HNO_3 into the dried residue, the beaker was sealed in a bomb and heated to 190 °C for 48 hr. Te coprecipitation was then carried out for further pre-concentration of PGE. Diluted aqua regia was then used to dissolve the Te precipitate and loaded on mixed ion exchange columns to remove interfering elements. The analysis was then carried out on an isotope dilution-ICP-MS at the SKLODG. Rh concentration was calculated by ^{194}Pt as an internal standard. The total blanks were 0.002 ppb for Ir, 0.012 ppb for Ru, 0.002 ppb for Rh, 0.040 ppb for Pd, and 0.002 ppb for Pt. WGB-1 and WPR-1 were also analyzed to control the experiment quality; the results are consistent with the recommend values (Qi et al., 2011).

Analytical method of the whole-rock Re–Os isotope has been previously reported by Chu et al. (2009). Two grams of powder and ^{187}Re-^{190}Os mixed spike were digested by reverse aqua regia in a Carius Tube
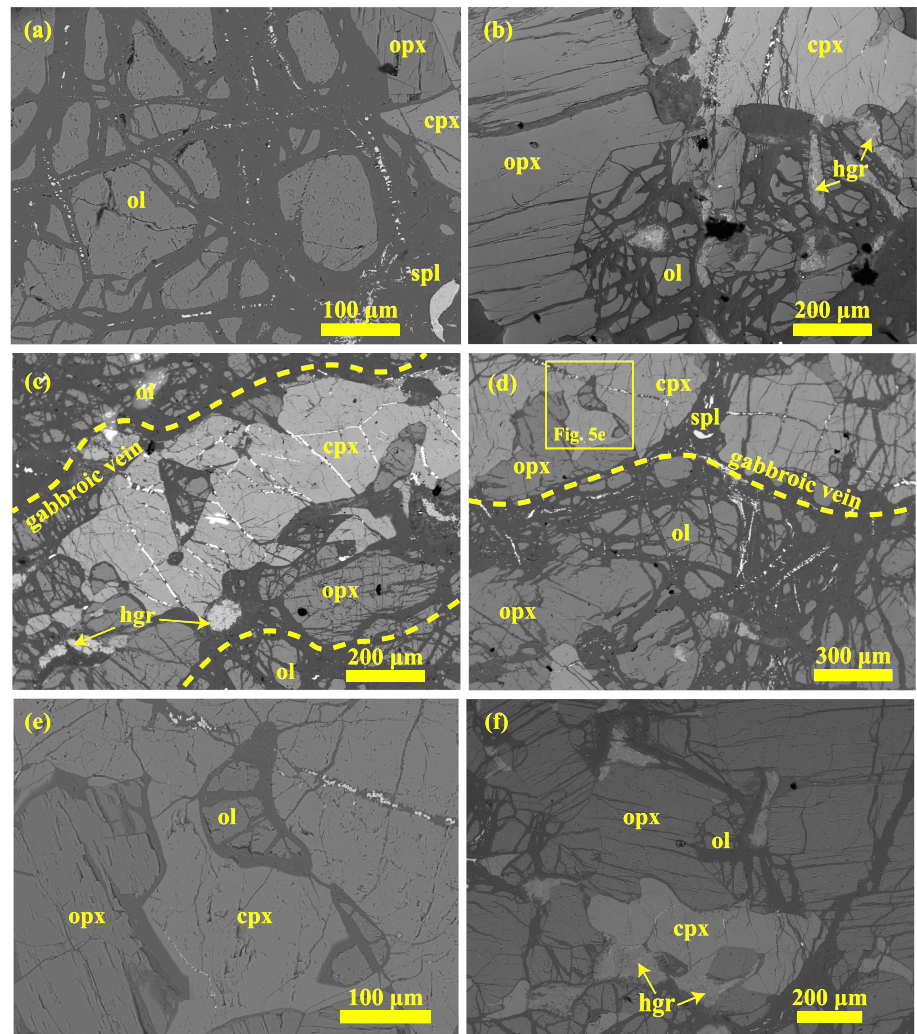
Figure 2. Back-scattered electron (BSE) images of the peridotites. (a) Harzburgites with porphyroclastic texture. (b) Melt impregnation evidence (e.g., crystallization of plagioclase and pyroxenes) in the harzburgites. Plagioclase is now altered to hydrogrossular. (c and d) Lherzolites with porphyroclastic texture being cut by websteritic veins. (e) A close up of gabbroic veins showing replacement of olivines by pyroxenes. (f) Interstitial clinopyroxene and plagioclase in the lherzolites. cpx = clinopyroxene; opx = orthopyroxene; ol = olivine; hgr = hydrogrossular = products of hydrothermal alteration of plagioclases.

at 240 °C for 72 hr. Os in aqua regia were extracted by CCl_4 (Cohen & Waters, 1996) and then further purified by microdistillation (Birck et al., 1997). Re that remained in the aqua regia was then purified by anion exchange separation techniques. Os isotope ratios were measured by Isoprobe-T Mass Spectrometer at the State Key Laboratory of Lithospheric Evolution, Institute of Geology and Geophysics, Chinese Academy of Sciences. The measurement was run in static mode using Faraday cups. Ba $(OH)_2$ was utilized as ion emitter for enhancing the ionization efficiency. Interference corrections, oxygen corrections, spike subtractions, and mass fractionation correction using $^{192}Os/^{188}Os = 3.08271$ were carried out on the measured Os isotopic ratios. The in-run precisions on $^{187}Os/^{188}Os$ of the analyses were better than $\pm 0.2\%$ (2σ). The Johnson–Matthey standard of University of Maryland (UMD) was employed as an external standard, and it returned the $^{187}Os/^{188}Os$ isotopic ratio of 0.11380 ± 4 (2σ, $n = 5$). Re was determined on a Neptune multicollector (MC)-ICP-MS. For all the samples, the in-run precisions were better than $\pm 0.5\%$ (2σ). Total analytical blanks were 2 pg for Re and 0.3–0.5 pg for Os with a $^{187}Os/^{188}Os$ ratio near 0.160. WPR-1 was analyzed as an unknown sample for data quality control, and the results are identical with the recommended value within analytical uncertainty for Os isotopic compositions, as well as Re and Os concentrations.

Table 1

Major Oxide and Selected Trace Element Composition of Peridotites From the Shuanggou Ophiolite

Sample No	SiO$_2$[a]	Al$_2$O$_3$	Fe$_2$O$_3$	CaO	MgO	Na$_2$O	K$_2$O	Cr$_2$O$_3$	TiO$_2$	MnO	P$_2$O$_5$	LOI	Total	Mg#[b]	Zr[c]	Y	Cr	Ni	Yb
Group-1 harzburgites																			
SG1111	38.69	2.03	6.55	0.51	36.96	<0.01	0.01	0.31	0.03	0.07	0	13.7	98.83	0.918	0.46	1.11	2170	1820	0.2
SG1112	38.26	2.61	7.3	0.02	36.72	<0.01	0.02	0.37	0.09	0.09	0	14.15	99.61	0.909	0.58	1.99	2318	1880	0.25
SG1313	39.22	1.64	7.48	0.03	37.23	0.05	<0.01	0.32	<0.01	0.11	<0.001	13.4	99.48	0.908	0.37	0.49	2128	2160	0.08
SG1317	41.38	1.17	7.57	0.31	35.77	0.05	<0.01	0.39	<0.01	0.07	0.01	13.1	99.82	0.903	0.58	0.57	3007	2200	0.09
SG1328	39.1	1.47	6.91	0.46	37.36	0.06	<0.01	0.41	<0.01	0.09	0	14	99.85	0.915	0.17	0.35	3155	1780	0.07
SG1329	38.93	2.44	7.91	0.13	36.24	0.05	0.01	0.36	0.05	0.07	0	13.4	99.58	0.901	1.52	0.55	2731	1830	0.04
SG1330	39.04	2.61	8.37	0.02	36.18	0.05	0.01	0.34	0.08	0.06	0	13.3	100.05	0.895	2.78	0.7	3314	1850	0.05
Group-2 harzburgites																			
SG1103	38.96	1.33	7.15	0.12	38.32	<0.01	0.01	0.31	<0.01	0.09	0	13.55	99.81	0.914	0.17	0.21	2064	1900	0.02
SG1314	38.05	0.61	7.34	0	38.65	0.06	<0.01	0.29	0.02	0.06	0	14.35	99.42	0.913	2.03	0.8	2371	2080	0.11
SG1326	39.25	0.58	6.73	0	38.64	0.05	<0.01	0.28	<0.01	0.06	0	13.8	99.38	0.919	0.28	0.08	2308	2010	0.01
SG1331	39.38	0.92	6.62	0	38.45	0.05	<0.01	0.32	<0.01	0.06	<0.001	14	99.78	0.920	0.32	0.1	3102	2040	0.02
SG1107	38.32	1.83	6.93	0.73	37.03	0.01	0.01	0.3	0.08	0.09	0	13.5	98.81	0.914	0.73	0.94	1789	1690	0.08
Plagioclase lherzolites																			
SG1320	39.44	2.39	7.81	1.47	35.6	0.07	<0.01	0.29	0.06	0.11	0	12.55	99.79	0.900	1.68	2.74	2297	1740	0.32
SG1321	39.38	2.28	8.15	1.73	35.79	0.08	0.01	0.35	0.08	0.12	0	12.15	100.1	0.897	1.98	0.92	2710	1710	0.06
SG1322	39.19	2.44	7.9	1.7	35.98	0.08	0.01	0.33	0.07	0.11	0	12.4	100.2	0.900	1.93	1.28	2477	1710	0.12
SG1323	39.81	1.99	7.96	1.49	36.29	0.07	0.01	0.27	0.06	0.1	0	12.15	100.2	0.900	2.15	1.44	2138	1770	0.15
SG1324	39.13	3.13	7.84	1.6	35.76	0.07	0.01	0.33	0.07	0.11	0	12.15	100.2	0.900	3.27	2.7	2858	1920	0.37

[a]Major oxides: wt.%.　　[b]Mg#: molar Mg/(Mg + Fe) in whole rock.　　[c]Trace elements: ppm.

4. Geochemical Compositions

For all the samples, whole-rock major and trace elemental compositions are given in Table 1, while whole-rock PGE compositions and $^{187}Os/^{188}Os$ ratios are listed in Table 2. According to the PGE compositions and $^{187}Os/^{188}Os$ ratios, the harzburgites can be separated into two groups (Figures 3 and 4). The Group-1 harzburgites are characterized by flat primitive upper mantle (PUM) normalized PGE patterns (e.g., $(Os/Ir)_N$: 0.85–1.25, $(Pd/Ir)_N$: 0.66–1.15), similar to typical abyssal/ophiolitic peridotites (Barnes et al., 1985, 2015) (Figure 3a). Two Group-1 harzburgite samples (SG1317 and SG1328) exhibit slight Pt and Pd enrichment ($(Pt/Ir)_N$: 1.27–1.34, $(Pd/Ir)_N$: 1.02–1.15). $^{187}Os/^{188}Os$ ratios of the Group-1 harzburgites vary from 0.12297 to 0.12727 (Figure 4) within the range of normal abyssal peridotites and are lower than the recommended value ($^{187}Os/^{188}Os = 0.1296 \pm 6$) of the PUM (Meisel et al., 2001). Re concentrations in the Group-1 harzburgites are very low, ranging from 0.05 to 0.17 ppb, with $^{187}Re/^{188}Os$ from 0.06 to 0.24. The Group-1 harzburgites have high MgO contents from 36.18% to 37.36% and Mg# from 0.895 to 0.918, but low Al$_2$O$_3$ contents from 1.17% to 2.61% and CaO contents from 0.02% to 0.51% (Table 1 and Figure 5).

The Group-2 harzburgites are characterized by highly variable PGE compositions and low $^{187}Os/^{188}Os$ ratios. PPGEs (palladium group PGEs: Rh, Pt, and Pd) exhibit different degrees of depletion or enrichment relative to IPGEs (iridium group PGEs: Os, Ir, and Ru), with variable PPGE/IPGE ratios (e.g., $(Pd/Ir)_N$: 0.33–1.78), possibly reflecting variable degrees of melt depletion or refertilization. The Group-2 harzburgites also exhibit significant fractionation in the IPGE group (e.g., $(Os/Ir)_N$: 1.14–5.05) (Figure 3b). Their $^{187}Os/^{188}Os$ ratios (0.11307–0.11651) are much lower than those of the Group-1 harzburgites (Figure 4). Meanwhile, the Group-2 harzburgites have more refractory whole rock compositions than the Group-1 harzburgites. Their MgO contents range from 37.03% to 38.65%, with high Mg# from 0.913 to 0.920. The two samples which show evidence of later melt impregnation (e.g., crystallization of pyroxene and plagioclase; Figure 2b) have higher CaO (0.12–0.73%) and Al$_2$O$_3$ contents (0.33–1.83%) than other harzburgites (CaO: <0.01%; Al$_2$O$_3$: 0.58–0.92%) (Figure 5).

In comparison with the harzburgites, the lherzolites are fertile in compositions, with lower MgO contents (34.83–37.03%) and Mg# (0.897–0.900) but higher Al$_2$O$_3$ (1.99–4.01%) and CaO contents (0.92–1.73%) (Figure 5), which is consistent with the presence of plagioclase and higher proportion of clinopyroxene. The lherzolites exhibit considerable IPGE fractionation in the PUM-normalized patterns. $(Os/Ir)_N$ varies from 1.76 to 2.16, which is within the range of the Group-2 harzburgites but higher than that of the

Table 2
HSE and Re-Os Isotopic Composition of Peridotites From the Shuanggou Ophiolite

Sample	Os[a]	Ir	Ru	Rh	Pt	Pd	Re	$^{187}Re/^{188}Os$	$^{187}Os/^{188}Os$	$(^{187}Os/^{188}Os)_i$[b]	T_{MA}[c]	T_{RD}
Group-1 harzburgites												
SG1111	3.46	3.63	7.16	1.00	6.67	4.89	0.101	0.141	0.12467	0.12377	1.05	0.70
SG1112	3.95	2.83	5.96	1.04	6.83	6.24	0.116	0.141	0.12727	0.12636	0.50	0.33
SG1313	3.94	3.93	7.37	1.15	6.59	5.62	0.048	0.058	0.12266	0.12228	1.14	0.98
SG1317	4.54	4.10	6.21	1.77	11.30	8.47	0.138	0.147	0.12297	0.12203	1.44	0.94
SG1328	4.19	3.11	5.41	1.52	9.04	7.23	0.138	0.159	0.12507	0.12405	1.03	0.64
SG1329	3.36	3.25	6.57	1.42	6.86	5.59	0.165	0.236	0.12385	0.12233	1.85	0.82
SG1330	3.09	3.34	6.44	1.46	7.53	7.01	0.131	0.204	0.12604	0.12473	0.98	0.51
Group-2 harzburgites												
SG1103	4.40	1.47	3.50	0.43	3.32	1.74	0.459	0.502	0.11651	0.11330	−10.48	1.84
SG1107	5.10	1.77	3.12	0.99	7.32	6.36	0.114	0.107	0.11631	0.11563	2.50	1.87
Duplicate	4.66						0.125	0.130	0.11697	0.11614	2.55	1.78
SG1314	4.15	3.27	9.43	1.06	1.42	2.22	0.046	0.053	0.11540	0.11506	2.28	2.00
SG1326	2.99	0.78	3.30	0.66	2.38	1.10	0.024	0.038	0.11307	0.11283	2.54	2.32
SG1331	5.60	1.00	1.62	0.65	5.53	3.43	0.057	0.049	0.11560	0.11528	2.22	1.97
Plagioclase lherzolites												
SG1320	3.12	1.60	3.62	1.12	6.35	5.29	0.216	0.334	0.12521	0.12307	2.98	0.62
SG1321	3.66	1.58	3.25	1.26	6.52	5.94	0.340	0.447	0.12666	0.12380	−6.83	0.42
SG1322	3.70	1.53	3.28	0.88	6.17	5.49	0.257	0.334	0.12538	0.12324	2.89	0.60
SG1323	4.07	1.79	3.65	1.11	6.20	5.77	0.227	0.269	0.12470	0.12298	1.92	0.70
SG1324	3.53	1.52	3.09	0.97	5.83	5.83	0.233	0.318	0.12518	0.12315	2.54	0.63

[a]HSE: ppb.   [b]Initial $^{187}Os/^{188}Os$ compositions are calculated by the age of 382.9 Ma (Jian et al., 2009b).   [c]Model ages (Ga) are calculated by using primitive upper mantle compositions ($^{187}Re/^{188}Os = 0.42$, and $^{187}Os/^{188}Os = 0.1296$; Meisel et al., 2001).

Group-1 harzburgites (Figure 3c). On the other hand, $(Pd/Ir)_N$ varies from 1.59 to 1.93, higher than that of the harzburgites. PGE patterns (except Re) of the lherzolites are highly consistent with the pattern of the sample SG1107, which belongs to the Group-2 harzburgites (Figure 3c). Os isotope ratios of lherzolites range from 0.12470 to 0.12753, similar to Os isotope ratios of Group-1 harzburgites and abyssal peridotites (Figure 4). On the other hand, lherzolites have relatively high Re concentrations (0.22–0.34 ppb) and $^{187}Re/^{188}Os$ ratios (0.27–0.45). Major and trace element compositions of clinopyroxenes from the lherzolites are listed in supporting information Table S1. In the rare earth element (REE) patterns, the clinopyroxenes are enriched in middle REE (MREE) relative to heavy REE (HREE), and depleted in light REE (LREE), which is different from clinopyroxenes in typical ophiolitic lherzolites (Figure 6a).

5. Discussion

5.1. Harzburgites: Different Mantle Origins

The Group-1 harzburgites exhibit overall flat PUM-normalized PGE patterns with nonchondritic PGE ratios, for example, Ru/Ir (1.51–2.11) and Pd/Ir (1.43–2.33) are higher than those of carbonaceous chondrites (e.g., Ru/Ir = 1.35, Pd/Ir = 0.45; Fischer-Gödde et al., 2010). These PGE features are similar to those in the ophiolitic and abyssal peridotites and have been proposed as indigenous features of the upper mantle (Becker et al., 2006; Liu et al., 2009). Meanwhile, Os isotope ratios of the Group-1 harzburgites also distributed within the range of typical abyssal peridotites (Figure 4). It is therefore suggested that the Group-1 harzburgites derived from the oceanic mantle in a ridge setting. In the Group-1 harzburgites, with the decrease of Al_2O_3 contents, Os concentrations increase while $^{187}Os/^{188}Os$ ratios decrease (Figures 7a and 7b), indicating that Os concentrations and isotope compositions in the Group-1 harzburgites were mainly controlled by the melting process (Lorand et al., 2013; Rudnick & Walker, 2009). The rhenium-depletion ages (T_{RD}) range from 0.33 to 0.74 Ga (Table 2). The age variation is caused by the remaining Re in the peridotites (Rudnick & Walker, 2009): the T_{RD} method assumes that no Re was retained in mantle peridotites after high degrees of melting and therefore no ^{187}Os has been generated since then. Consequently, this approach would underestimate the true melt depletion ages and provide a wide range of ages if a certain amount of Re remains in the peridotites after melt extraction. Thus, the age of 0.74 Ga is the minimum estimate of the true melt depletion age.
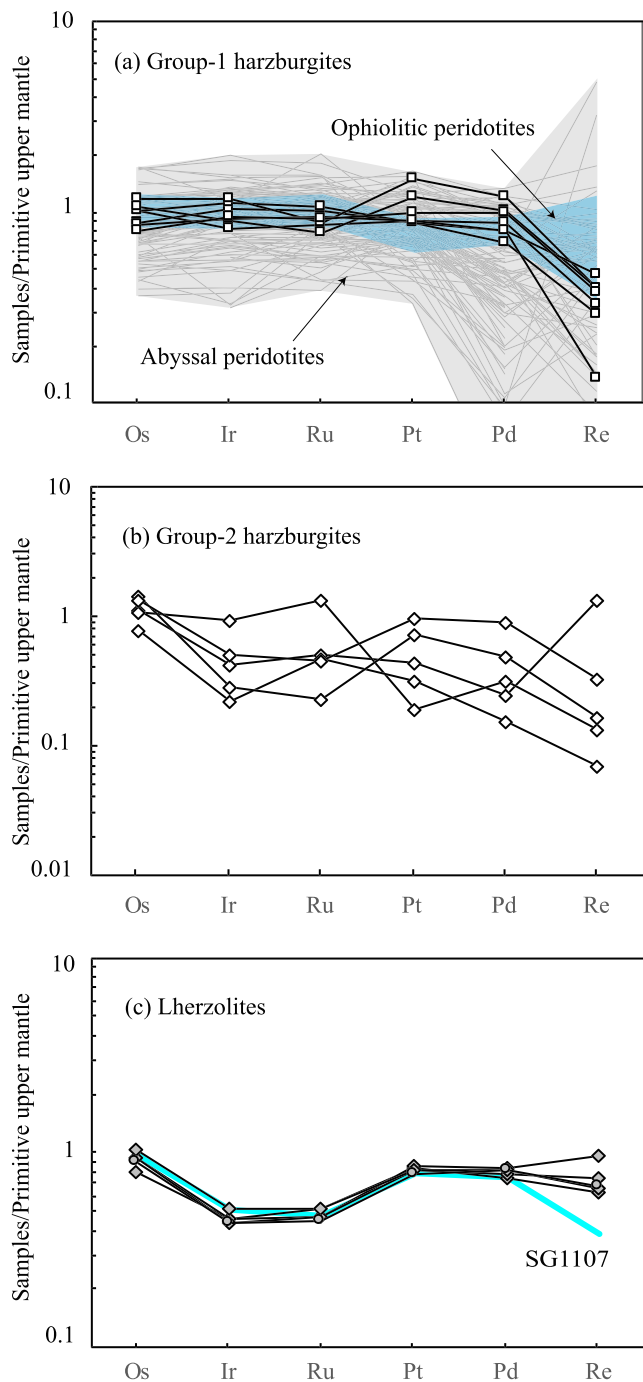
Figure 3. Primitive upper mantle normalized PGE diagrams for the (a) the Group-1 harzburgites, (b) the Group-2 harzburgites, and (c) the lherzolites from the Shuanggou ophiolite. The normalization values are from Becker et al. (2006) and Fischer-Gödde et al. (2011). Data of the ophiolitic peridotites are from Becker et al. (2006) and Fischer-Godde et al. (2011), while data of abyssal peridotites are after the compilation by Day et al. (2017) (three highly fractionated samples are excluded).

The Group-2 harzburgites have more refractory whole rock compositions and much lower $^{187}Os/^{188}Os$ ratios than the Group-1 harzburgites. PGE compositions are also very different from the Group-1 harzburgites (Figure 3b). The depletion of PPGE relative to IPGE and the more refractory whole-rock compositions of the Group-2 harzburgites indicate a large degree of melting during which the PPGE-enriched sulphide were extracted from the mantle (Lorand et al., 2013). Meanwhile, fractionation within the IPGE group (e.g., Os, Ir and Ru) is not common in ophiolitic and abyssal peridotites. Volatile-rich, small volume melts can cause fractionation of Os relative to Ir (e.g., Alard et al., 2011). However, this explanation is not acceptable, as the Group-2 harzburgites have very low Os isotope ratios. Alternatively, the fractionation between Os and Ir could be a result of large degree of melting (Wang et al., 2013), during which the extraction of sulfur into silicate melt leads to decrease in fS_2 and further exsolution of Os-rich alloys (i.e., osmiridiums) in the residue (Fonseca et al., 2012). Therefore, fractionation of the compatible highly siderophile elements (HSE) in melting residues will be controlled by the different solubilities of these elements in the Os-rich alloys (Brenan & Andrews, 2001). Another explanation of the IPGE fractionation is that these signatures define a special mantle reservoir that has different PGE compositions to the primitive upper mantle. Most importantly, the Group-2 mantle harzburgites have very low Os isotope ratios (Table 2 and Figure 4). The Os isotope model age indicates that the Group-2 harzburgites experienced mantle melting in Paleoproterozoic (T_{RD}: 1.98–2.28 Ga). In summary, all these features above indicate that the Group-2 harzburgites represent ancient refractory mantle domains that have been preserved in the oceanic lithosphere (e.g., Harvey et al., 2006; Liu, Snow, et al., 2008).

5.2. Lherzolites: Records of an Ancient Refertilization Process
5.2.1. Petrogenesis of Lherzolites: Refertilization or Subsolidus Recrystallization

Lherzolites containing plagioclase can be generated by two different processes: (1) melt refertilization of refractory peridotites (Arai, 1991; Rampone et al., 1997; Liu et al., 2010); and (2) subsolidus recrystallization of spinel peridotites under plagioclase facies conditions (Cannat & Seyler, 1995; Hamlyn & Bonatti, 1980). The Shuanggou lherzolites in this study exhibit clear evidence of melt refertilization. First, in the lherzolites, the porphyroclastic assemblage has partially been replaced or cut by a second generation of veins or pockets which are composed of pyroxene and a smaller portion of plagioclase (Figure 2). The plagioclases commonly form as small grains with texture evidence of cocrystallization with clinopyroxene. The petrographic evidence eliminates the possibility that the plagioclases in the Shuanggou lherzolites formed by spinel breakdown in a closed system but does support its formation through the process of melt refertilization. Second, the lherzolites have high CaO and Al_2O_3 contents relative to the harzburgites (Figure 5). Such chemical variations can be best explained by a latter refertilization process in an open system rather than by a spinel break-up process in a closed system.

Several facts demonstrate that the lherzolites were transformed from the Group-2 harzburgites. First, in terms of petrology, only the Group-2 harzburgites exhibit features of melt impregnation, while the Group-1 harzburgites completely lack these features (Figure 2). Second, in terms of PGE geochemistry, during mantle melting, IPGE (Os, Ir, and Ru) are stored in the mantle residue, but the PPGE (Pt and
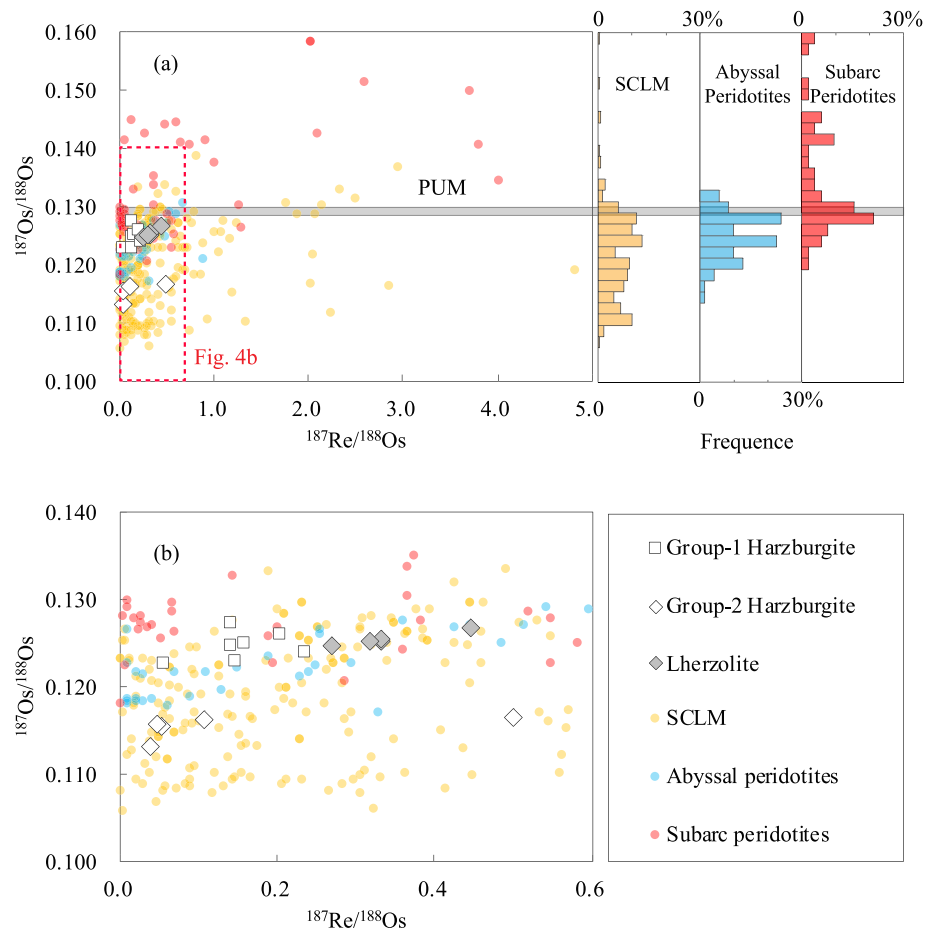
Figure 4. (a) Re-Os isotope compositions of the Shuanggou peridotites and literature data. Some peridoites may have high $^{187}Re/^{188}Os$ ratios so that they are not shown in the $^{187}Re/^{188}Os$-$^{187}Os/^{188}Os$ diagram, but their $^{187}Os/^{188}Os$ are still included in the frequency histograms. (b) A close up of Re-Os isotope compositions. The data of the abyssal peridotites are from Alard et al. (2005), Brandon et al. (2000), Harvey et al. (2006), Liu et al. (2008), and Snow and Reisberg (1995). The data of SCLM xenoliths are from Becker et al. (2006), Chesley et al. (1999), Meisel et al. (1996, 2001), Fischer-Gödde et al. (2011), Ionov et al. (2006, 2015, 2015), Pearson et al. (2004), Pernet-Fisher et al. (2015), and Sun et al. (2017). The data of subarc peridotites are from Brandon et al. (1996), Widom et al. (2003), and Saha et al. (2005). $^{187}Os/^{188}Os$ of the primitive upper mantle (PUM) is 0.1296 according to Meisel et al. (2001)

Pd) and Re will be extracted by the melts (Lorand et al., 2013). Thus, mantle-derived melts are commonly enriched in Re and PPGE relative to IPGE. Refertilization by these melts will increase PPGE and Re compared with IPGE in the peridotites but hardly cause fractionation within the IPGE group (e.g., Os/Ir) (e.g., Lorand et al., 2009; Rehkaemper et al., 1999). The lherzolites exhibit considerable Os-Ir-Ru fractionation, which is similar to the Group-2 harzburgites but different from the Group-1 harzburgites, indicating that their protolith are the Group-2 harzburgites. Moreover, the PGE patterns of the lherzolites are very similar to that of sample SG1107 (Figure 3c), which belongs to the Group-2 harzburgites and exhibits feature of low-degree melt impregnation. In addition, $^{187}Os/$ ^{188}Os compositions of the lherzolites are much different from those of the Group-2 harzburgites. The effect of refertilization on Re-Os isotope system will be discussed in section 5.2.3, after a discussion about the percolating melt in section 5.2.2.

5.2.2. Composition of the Percolating Melt

As revealed by Zhou et al. (1995), the gabbroic veins/pockets in the Shuanggou lherzolites have chondritic Nd isotopic compositions ($\varepsilon_{Nd}(t) = -1$ to $+3$). In contrast, the associated mafic crust as represented by diabases have much higher $\varepsilon_{Nd}(t)$ ratios from $+9.7$ to $+11.6$, that are in the range of the upper oceanic mantle (Hu et al., 2015). This isotope inconsistency is not common in the magma-poor rifted margins, in which
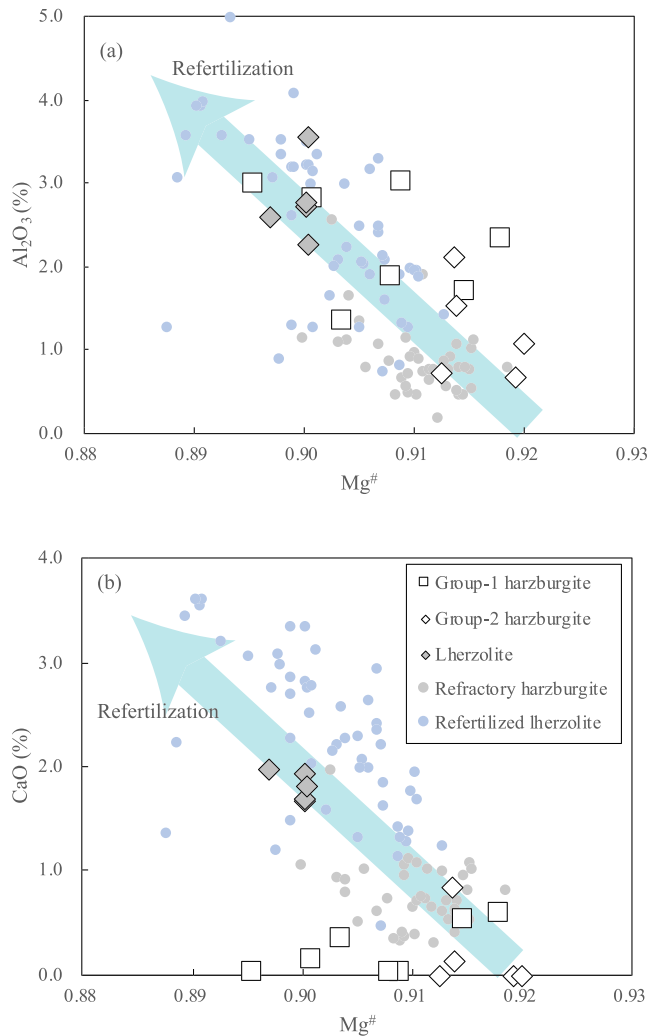
Figure 5. Major element compositions of the Shuanggou peridotites. (a) Mg# versus Al$_2$O$_3$ and (b) Mg# versus CaO. Major element composition of refractory harzburgites and refertilized lherzolites are from Le Roux et al. (2007), Takazawa et al. (2000), and Ionov et al. (2005).

clinopyroxenes in the plagioclase lherzolites have Nd isotopic compositions identical to the associated mafic crust (e.g., Müntener et al., 2004). Instead, the isotope inconsistency implies that the melts, which impregnated the peridotites and produced the gabbroic veins/pockets, derived from a source different from that of the diabases. For example, the percolating melt might be derived from a subarc mantle or a mantle plume.

To further investigate the percolating melt, REE concentrations of clinopyroxenes were used. Comparison of chondrite-normalized REE patterns of clinopyroxenes between different types of rocks is shown in Figure 6. The clinopyroxenes in the Shuanggou lherzolites exhibit upward convex REE patterns, with enrichment in MREE relative to HREE and slight depletion in LREE. Clinopyroxenes in the lherzolites in classic continental extensional settings have been interpreted as products of percolating melt; however, their REE patterns are characterized by LREE-depletion relative to HREE (Le Roux et al., 2007; Müntener et al., 2004) (Figure 6a). Clinopyroxenes in abyssal peridotites have highly variable REE compositions with patterns from LREE-depleted to LREE-enriched patterns (Warren, 2016, and references therein), while clinopyroxenes in subarc mantles have relatively lower REE concentrations with overall LREE-depleted patterns (Bizimis et al., 2000; Parkinson & Pearce, 1998). Clearly, neither abyssal peridotites nor subarc mantle peridotites comprise clinopyroxenes with REE patterns similar to those of the Shuanggou lherzolites. In contrast, clinopyroxenes from plume-related lavas have upward convex REE patterns like the Shuanggou lherzolites (Kamenetsky et al., 2012) (Figure 6b).

Dy and Yb concentrations in clinopyroxenes can serve as useful parameters to distinguish clinopyroxenes of different tectonic settings (Jean et al., 2010; Le Roux et al., 2014). Because of larger-degree flux melting in the mantle wedge, clinopyroxenes in the subarc mantle generally have lower Dy and Yb concentrations than clinopyroxenes in the abyssal peridotites (Figure 8). Clinopyroxenes in the Shuanggou lherzolites have higher Dy and Yb concentrations than those in the subarc peridotites, while have lower Yb concentrations than those in the abyssal peridotites at given Dy concentrations. In this diagram, clinopyroxenes in the Shuanggou lherzolites plot near the range of the mantle plume area (Kamenetsky et al., 2012) (Figure 8). We then calculated REE compositions of the percolating melt using clinopyroxene-melt partition coefficients estimated by Sun and Liang (2012) (Figure 9). The calculated REE compositions are much different from the Shuanggou diabases and mid-ocean ridge basalts (MORBs) but are very similar to oceanic island basalts (OIB). Therefore, together with the chondritic Nd isotopes of the gabbroic veins/pockets (Zhou et al., 1995), it is proposed that the percolating melt have compositions close to plume-related magmas, which are clearly different from diabases in the Shuanggou ophiolite.

5.2.3. Ancient Refertilization Process Revealed by Re-Os Isotope

The effect of refertilization on the Re–Os isotope system relate to three factors: (1) compositions of the melt and rock, (2) melt/rock ratios, and (3) the time of the process. The first and second factors control the isotope variation during the melt-rock reaction, while the third factor affects the subsequent isotope evolution. As mentioned above, the lherzolites in this study were formed through melt impregnation into the Group-2 harzburgites, which represent an ancient depleted mantle domain. However, these lherzolites exhibit much higher ^{187}Os/^{188}Os ratios than the Group-2 harzburgites. Because of the low concentrations of Os in silicate melts relative to the mantle residues, the large Os isotope variation cannot be simply explained by addition of melts into the Group-2 harzburgites at the time of ocean formation (~0.4 Ga), as is illustrated by the mass equilibrium calculation (Figure 7b). It should be noted that, in some cases, peridotites after large degree of melt modification, for example, dunite in the spreading center, could have higher ^{187}Os/^{188}Os but
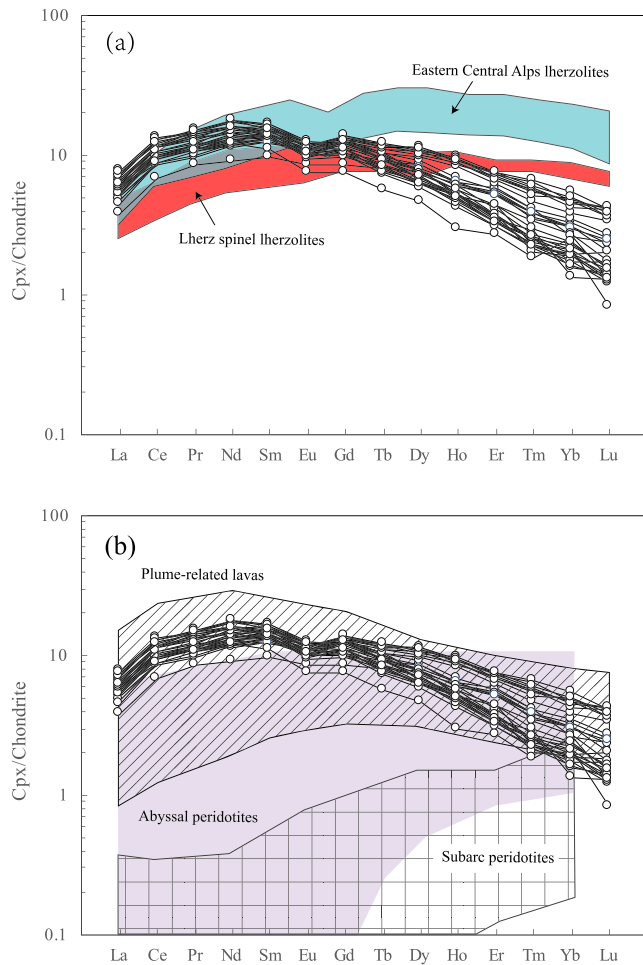
Figure 6. Chondrite-normalized REE diagrams of the clinopyroxenes in the lherzolites in comparison with (a) clinopyroxenes in lherzolites in classic continental extensional domains and continent-ocean transitions (Le Roux et al., 2007; Müntener et al., 2004) and (b) clinopyroxenes in abyssal peridotites (Warren, 2016, and references therein), subarc mantle peridotites (Bizimis et al., 2000; Parkinson & Pearce, 1998), and plume-related lavas (Kamenetsky et al., 2012).

significantly lower Os contents than their protolith if the primary sulfides were removed (e.g., Buchl et al., 2002). However, in our study, there is no evidence of Os-loss during the refertilization process, and it is still difficult to explain why the Group-2 harzburgite sample SG1107 has similar PGE compositions but low $^{187}Os/^{188}Os$ ratios in comparison to the lherzolites.

When the refertilization took place tends to be more important for the variation of Os isotopes. Regarding the large difference of the Os isotopes between the lherzolites and the Group-2 harzburgites, a reasonable explanation is that the Os isotope difference are due to combination of (1) the mantle refertilization and (2) postrefertilization, long-period daughter isotope growth. During mantle melting and refertilization, Re is controlled by silicate melts rather than sulphides. Thus, Re and PGE may be decoupled and enriched to different extents during the refertilization process. Although mantle refertilization only slightly affected the $^{187}Os/^{188}Os$ ratios of the protolith, it could cause certain increase of $^{187}Re/^{188}Os$ ratio. Therefore, after a long time, there will be large differences in Os isotopes between the lherzolites and their protolith.

Re concentrations of the lherzolites are higher than those of the harzburgites, and show positive correlation with CaO, confirming that Re has been enriched during the refertilization (Figure 10a). The Group-2 harzburgites, with low CaO and Re contents, have low $^{187}Os/^{188}Os$ ratios, while lherzolites, with high CaO and Re contents, have high $^{187}Os/^{188}Os$ ratios. This variation supports the view that the difference of $^{187}Os/^{188}Os$ between the harzburgites and the lherzolites are related to their different $^{187}Re/^{188}Os$ ratios after the refertilization. However, Re concentrations and $^{187}Re/^{188}Os$ ratios may be affected by the serpentinization process. Therefore, the effect of serpentinization on the Re-Os isotope system needs to be evaluated. The serpentinization process has negligible effects on Os (Burnham et al., 1998; Chen & Xia, 2008; Dai et al., 2011; Harvey et al., 2006; O'Driscoll et al., 2012; Schulte et al., 2009), because the process proceeds under the reducing condition that tend to stabilize HSE-bearing phases (Buchl et al., 2002; Evans et al., 2013; Hyndman & Peacock, 2003; Mével, 2003; Snow & Reisberg, 1995). In comparison, the behavior of Re during serpentinization is still unclear (Schulte et al., 2009). Some studies found that Re might have been moderately enriched by serpentinization (e.g., Harvey et al., 2006), whereas others argued that no solid correlations exist between Re content and serpentinization intensity (e.g., Liu, Snow,

et al., 2008). In this study, the ratios of Re/Yb and Zr/Yb are introduced to constrain the Re behavior during the serpentinization process, since Re and Yb have similar compatibility during magmatic processes in mafic systems (Hauri & Hart, 1997; Reisberg et al., 2008) and Zr and Yb are immobile in the alteration processes. As shown in Figure 10b, all the lherzolite samples exhibit a good positive relation between Re/Yb and Zr/Yb, illustrating that Re in the lherzolites is not mobile during the serpentinization process. In comparison, the data of harzburgites are scattered, this is because that the harzburgite also experienced larger degrees of serpentinization. The preservation of the Re in the lherzolites is because that Re is mainly host in gabbroic veins that are resistant to hydrothermal alteration.

$^{187}Os/^{188}Os$ ratios of the lherzolites at different ages are calculated and then compared with the mixing result of the Group-2 harzburgites and the assumptive melts (Figure 7b). To estimate the minimum age of refertilization, we assume a melt with high Os concentrations and high $^{187}Os/^{188}Os$ ratio. For comparison, a melt with low Os concentrations are also used. According to mass equilibrium, the present data suggest that the refertilization took place at least 1.5 Ga (Figure 7b). On the other hand, Os isotope evolutionary history of the lherzolites is illustrated in Figure 11, assuming that (1) no ^{187}Os has been generated in the Group-2 harzburgites after the large-degree melt depletion and (2) $^{187}Os/^{188}Os$ ratio only slightly increased during melt
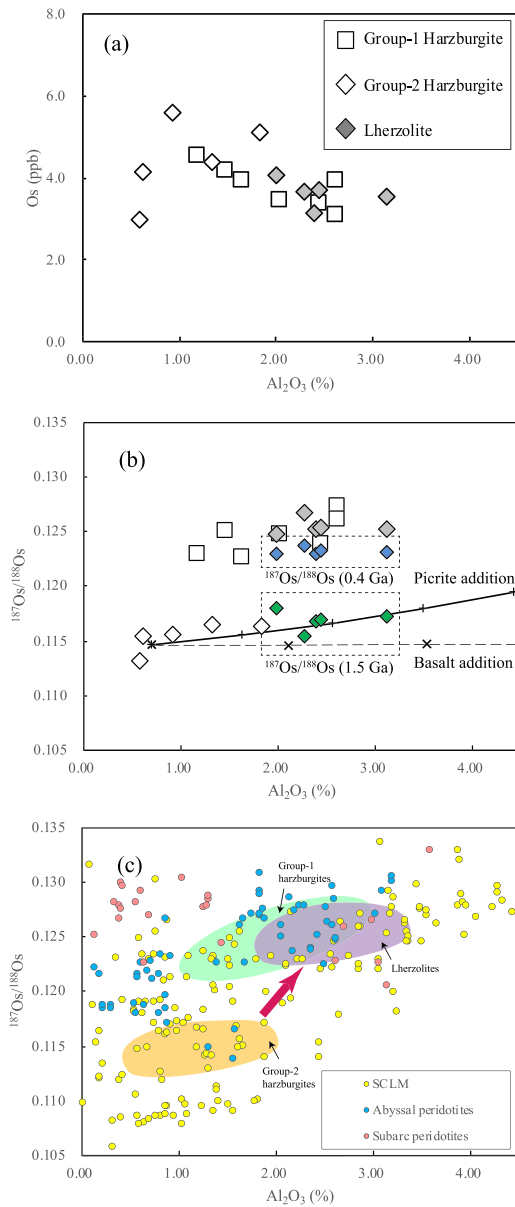
Figure 7. (a) Os variations with respect to Al_2O_3. (b) Correlations between Al_2O_3 and $^{187}Os/^{188}Os$ in the Shuanggou peridotites. Refertilization of the Group-2 harzburgites by addition of picritic (upper curve) or basaltic melt (lower curve) is illustrated. Mixing parameters: picritic melt has 1 ppb Os, 10 wt.% Al_2O_3, and an $^{187}Os/^{188}Os$ of 0.15; basaltic melt has 50 ppt Os, 15 wt.% Al_2O_3, and an $^{187}Os/^{188}Os$ of 0.15. Tick marks on both curves represent increments of 10% melt addition. Os isotope ratios at 0.4 and 1.5 Ga of the lherzolites are also present in blue and green diamonds, respectively. (c) Comparison between the Shuanggou peridotites and abyssal peridotites and xenoliths of subcontinental lithospheric mantle (SCLM). The data of the Shuanggou peridotites are exhibited as areas of different colors (green: Group-1 harzburgites; orange: Group-2 harzburgites; purple: lherzolites). The data of the abyssal peridotites are from Alard et al. (2005), Brandon et al. (2000), Harvey et al. (2006), Liu et al. (2008), and Snow and Reisberg (1995). The data of SCLM xenoliths are from Becker et al. (2006), Chesley et al. (1999), Meisel et al. (1996, 2001), Fischer-Gödde et al. (2011), Ionov et al. (2006); Ionov, Carlson, et al. (2015); Ionov, Doucet, et al. (2015); Pearson et al. (2004), Pernet-Fisher et al. (2015), and Sun et al. (2017). The data of subarc peridotites are from Brandon et al. (1996), Kepezhinskas et al. (2002), Widom et al. (2003), and Saha et al. (2005).

refertilization. The growth of $^{187}Os/^{188}Os$ accelerated after the increase of $^{187}Re/^{188}Os$. Therefore, the T_{MA} model ages, which are determined by the intersection of the $^{187}Os/^{188}Os$ evolution of the sample and a model mantle evolution curve, should provide upper limit of the true age of the refertilization process (Figure 11). For the lherzolites, the T_{MA} ages range from 1.92 to 2.89 Ga. Together with the T_{RD} (1.78–2.38 Ga) and T_{MA} (2.22–2.55 Ga) model ages of the Group-2 harzburgites, which underestimate the depletion age of the protolith, the refertilization process most likely took place at a very ancient time, possibly between 1.5 and 1.9 Ga.

5.3. The Origin of Ancient Refractory Mantle

The above discussion suggests that (1) the percolating melt have isotope and REE compositions close to plume-related lavas (e.g., OIB) but very different from the diabases in the Shuanggou ophiolite which show isotope and chemical compositions similar to N-MORB, and (2) the refertilization process which converted the Group-2 harzburgites to the lherzolites took place much earlier than the mantle exhumation process associated with the ocean formation. Therefore, the formation of the Shuanggou lherzolites is clearly disconnected from the mantle exhumation process at the time of continental rifting (~0.4 Ga), which is different from the classic model of lherzolites in the magma-poor rifted margins (e.g., Müntener et al., 2004, 2010).

Further interpretation of the ancient refertilization process should take the origin of the ancient refractory mantle domain into consideration. Ancient refractory mantle domains have been widely identified in abyssal and orogenic peridotites (Alard et al., 2005; Bizimis et al., 2007; Cipriani et al., 2004; Coltorti et al., 2010; Harvey et al., 2006; Liu, Snow, et al., 2008; Rampone & Hofmann, 2012; Stracke, 2008; Warren et al., 2009). These refractory domains could be either (1) ancient depleted mantle preserved in the convective mantle (e.g., Liu, Snow, et al., 2008) (Figure 12a) or (2) subcontinental lithospheric mantle (SCLM) incorporated in the upwelling asthenosphere during continental rifting and break-up (e.g., O'Reilly et al., 2009) (Figure 12b).

In the first hypothesis, refractory domains could have been survived from erasure by mantle convection in a long time (Figure 12a) (Liu, Snow, et al., 2008). The refractory domains make only small contribution to the genesis of the MORB, but fertile mantle can have a closer genetic relation to the MORB. Our study may have illustrated that the fertile mantle rocks that formed at a very ancient time can also be preserved for a long time in the mantle convection system. The involvement of these ancient fertile domains should play an important role in the upper mantle heterogeneity and the magma genesis.

To our knowledge, the abyssal peridotite samples with ancient depletion signals are always found at slow and ultra-slow spreading ridge settings. This may support the second hypothesis (Figure 12b), that the refractory mantle represents SCLM trapped by the upwelling asthenosphere, given that rocks from slow spreading ridges share many similarities with mantle tectonites exhumed in passive continental margin or transitional oceanic environments (Becker & Dale, 2016). However, sample bias must be taken into consideration, because slow spreading ridges expose more peridotite samples on average and have received more attention from researchers (Becker & Dale, 2016). Meanwhile, slow spreading
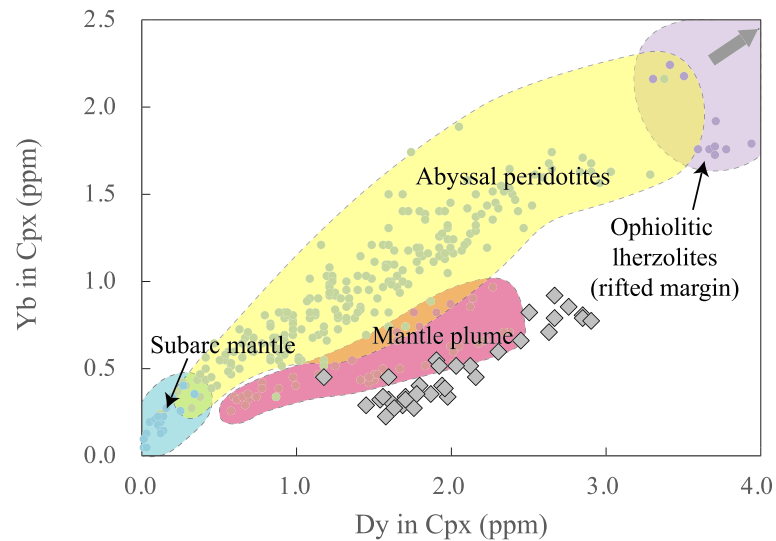
Figure 8. Yb versus Dy concentrations (in ppm) in clinopyroxene in the Shuanggou lherzolites in comparison with clinopyroxenes from different tectonic settings. The data source is the same as that of Figure 6.

ridges can also occur in well-developed ocean basins (e.g., Mid-Atlantic Ridge; Sempéré et al., 1993). Therefore, this point does not well constrain that the refractory domain derived from SCLM. In the following discussion, we provide several lines of evidence to support the view that the refractory domain (i.e., Group-2 harzburgites and lherzolites) in the Shuanggou mantle peridotites represents an isolated slice of SCLM.

First, REE compositions of clinopyroxenes in the Shuanggou lherzolites do not overlap with those in the abyssal peridotites (Figure 6b). Although REE patterns of clinopyroxenes in abyssal peridotites are highly variable, none of them exhibit upward convex REE pattern like the Shuanggou lherzolites. In particular, clinopyroxenes in the abyssal lherzolites always have LREE-depleted patterns (Warren, 2016). Indeed, the

Figure 9. Calculated REE concentrations of the percolating melts (solid black lines) in equilibrium with clinopyroxene in the Shuanggou lherzolites. Distribution coefficients were calculated according to the major composition of the clinopyroxenes at 1400 °C (Sun & Liang, 2012). Solid red, blue, and green lines are rare earth element concentrations of OIB, E-MORB, and N-MORB (Sun & McDonough, 1989). Dashed brown and orange lines are rare earth element concentrations of average oceanic arc lavas and continental arc lavas from Kelemen et al. (2003). Data of the Shuanggou diabases is from Hu et al. (2014).
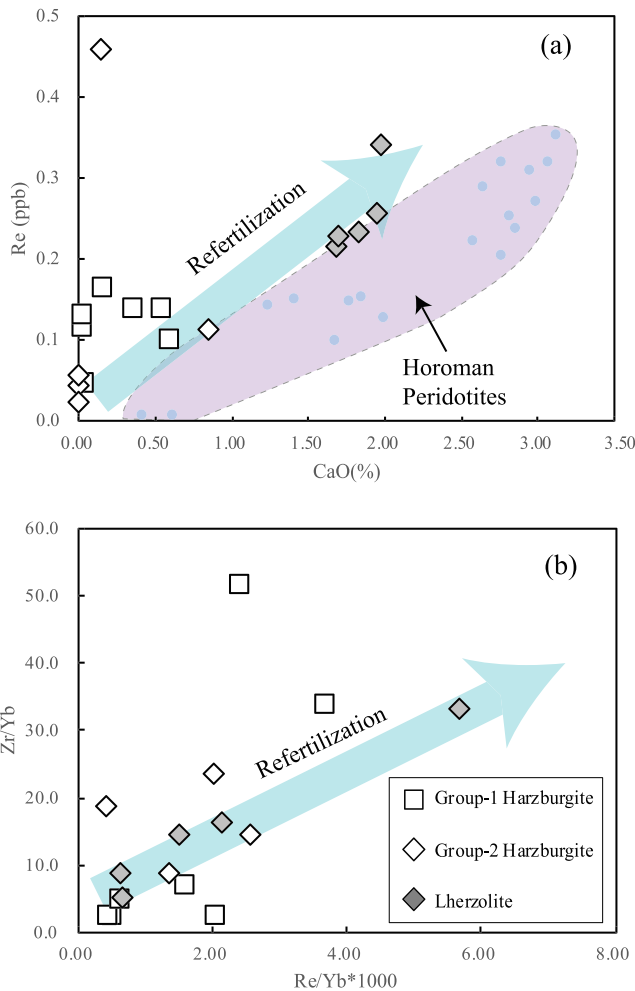
Figure 10. (a) CaO versus Re, and (b) Re/Yb versus Zr/Yb. A series of gradually refertilized Horoman peridotites from refractory harzburgite to fertile plagioclase lherzolites are exhibited in order to illustrate the effect of refertilization on CaO and Re. The data of the Horoman peridotites are from Takazawa et al. (2000) and Saal et al. (2001).

upward convex REE pattern has been identified in several SCLM xenoliths. For example, lherzolite xenoliths in the Siberian SCLM craton after plume modification contain clinopyroxenes with the upward convex REE patterns (Pernet-Fisher et al., 2015; Sun et al., 2017).

Second, osmium isotope variation with chemical fertility indexes (e.g., Al_2O_3) is a potential tool to determine the origin of the refractory mantle (Lassiter et al., 2014; Liu et al., 2019). Because Al_2O_3 has bulk partition coefficients similar to Re in most igneous processes, its relationship with $^{187}Os/^{188}Os$ (alumina-chrons) has been widely used to constrain the depletion age of mantle peridotites (Rudnick & Walker, 2009). For example, orogenic peridotites from the Ronda and Eastern Pyrenean ultramafic massifs show positive linear relations between $^{187}Os/^{188}Os$ ratios and whole-rock Al_2O_3 contents, providing model ages close to the Nd model ages of the associated lower crust; this finding suggested that the Ronda and Eastern Pyrenean peridotites represent SCLM which was isolated from the convecting mantle (Reisberg & Lorand, 1995). A further compilation of SCLM xenoliths provide a steep correlation, even including those xenoliths that have been metasomatized by melts or fluids (Becker et al., 2006; Chesley et al., 1999; Fischer-Gödde et al., 2011; Ionov et al., 2006, 2015, 2015; Meisel et al., 1996, 2001; Pearson et al., 2004; Sun et al., 2017) (Figure 7c). In comparison, most global abyssal peridotite data exhibit a positive and flatter trend with higher y intercept (Alard et al., 2005; Brandon et al., 2000; Harvey et al., 2006; Liu, Snow, et al., 2008; Snow & Reisberg, 1995). Exceptionally, three abyssal peridotites with the lowest $^{187}Os/^{188}Os$ ratios from the Gakkel Ridge do not have the lowest whole-rock Al_2O_3 concentrations (Liu, Snow, et al., 2008), and therefore deviate from the trend of the abyssal peridotites but plot within the range of SCLM xenoliths (Figure 7c). The difference in $^{187}Os/^{188}Os$-Al_2O_3 trends between abyssal peridotites and SCLM xenoliths are best explained by their different melt extraction history. In Figure 7c, it is evident that the Group-2 harzburgites and lherzolites in the Shuanggou ophiolite together define a steep relation similar to that of SCLM xenoliths, and more importantly, all the Group-2 harzburgites plot within the area of SCLM xenoliths. These facts support an SCLM affinity for the Group-2 harzburgites.

Third, the "SCLM-origin" explanation is more consistent with the history of the Yangtze Block. On the one hand, the detrital zircons from the western Yangtze Block exhibit a peak at 2.35–2.25 Ga (Zhao et al., 2010), which is consistent with the Os model age of the Group-2 harzburgites. On the other hand, between 1.9 and 1.5 Ga, the Yangtze Block was a part of the supercontinent Nuna/Columbia. The global anorogenic magmatism related to the cycle of the supercontinent at that time fulfilled the conditions of the ancient refertilization by OIB-like melts (Zhao et al., 2002). Indeed, mafic rocks in this period with OIB-like signature have been widely reported in the western Yangtze Block (e.g., Fan et al., 2013; Lu et al., 2019).

Therefore, based on all the evidence above, the refractory mantle domain (i.e., the Group-2 harzburgites) in the Shuanggou ophiolite most likely represent slices of SCLM that has been trapped by upwelling asthenospheric mantle (represented by the Group-1 harzburgites) during continental rifting and break-up. At that time, fertile mantle domains of the SCLM (i.e., the Shuanggou lherzolites) could be trapped by the asthenospheric mantle as well.

5.4. Plagioclase Peridotites and Fertile Mantles of Different Ages

Plagioclase peridotites account for a considerable portion (~30 vol%) of abyssal peridotites and ophiolitic mantle peridotites (Pirnia et al., 2018). These rocks mainly occur in the lithospheric mantle in extensional
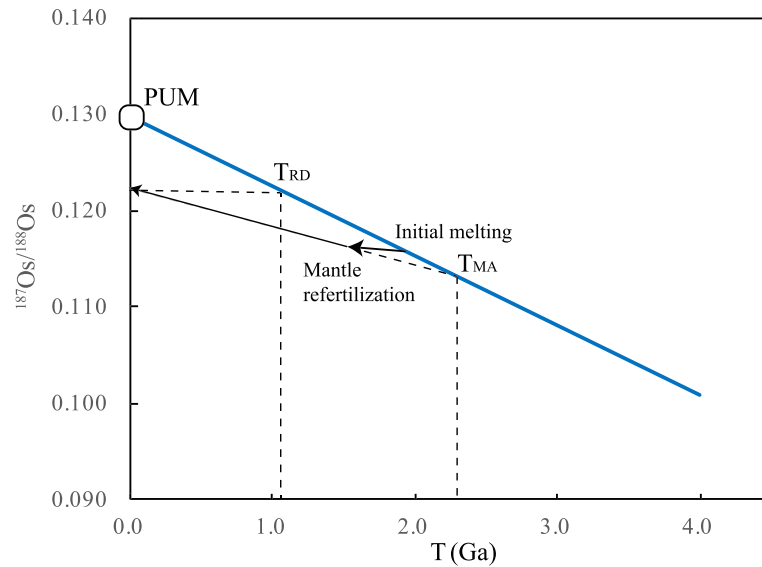
Figure 11. Osmium isotope evolution in the lherzolites through the melt depletion and the mantle refertilization.

settings. Therefore, except a smaller portion of plagioclase peridotites which were formed by subsolidus recrystallization of peridotites under plagioclase facies conditions (e.g., Hamlyn & Bonatti, 1980), most plagioclase peridotites have been proposed as important indicators of melt-rock interaction during lithospheric extension (Dick, 1989; Müntener et al., 2004, 2010; Pirnia et al., 2018; Rampone et al., 2009). However, in the case of the Shuanggou ophiolite, the refertilization process that converted the harzburgites into the lherzolites is clearly disconnected from the mantle exhumation process at the time of continental rifting, because (1) the percolating melt have isotope and REE compositions different from the diabases in the Shuanggou ophiolite, and (2) the refertilization process took place much earlier (1.5–1.9 Ga) than the mantle exhumation process associated with the ocean formation (~0.4 Ga). Our study therefore highlights that using plagioclase peridotites to constrain melt-rock process during continental breakup and seafloor spreading should be approached with caution, because some plagioclase peridotites might form in ancient times.

The above discussion also indicates that the Shuanggou lherzolites represent ancient fertile SCLM domain that has been trapped by upwelling asthenosphere (Figure 12b). Refertilization via melt addition can cause critical changes in physical properties of ancient SCLM, including viscosity reduction and density increase (Foley, 2008; Lee et al., 2011; Tang et al., 2013). Due to the change in physical properties, the refertilized areas are important rheologically weak domains in the lithosphere. This means that local destabilization and further removal of the lithosphere mantle take place more readily in the refertilized area (Le Roux et al., 2007; Zheng et al., 2015). Therefore, the refertilized area could have more chance to interact with or be incorporated by the upwelling asthenosphere during the continent-ocean transition.

Besides, this study also confirms that refertilization can take place episodically or continuously in the mantle (Le Roux et al., 2016). Fertile mantle rocks like the Shuanggou lherzolites and some layered websterites from the Lherz massif (France) is related to mantle refertilization processes much earlier than the exhumation process (Le Roux et al., 2016; this study), while genesis of many other fertile mantle rocks is strongly related to the exhumation process (Dick, 1989; Müntener et al., 2004, 2010; Rampone et al., 2009). Mantle refertilization process thus can create fertile mantle domains of different ages, which will evolve toward different isotope compositions due to postrefertilization isotope growth. In comparison with fertile mantle domains that formed at the exhumation stage, domains formed by ancient refertilization process have enough time for isotopic evolution. Take the Shuanggou ophiolite as an example, after more than one-billion-year evolution, the Shuanggou lherzolites have more radiogenic isotope compositions ($^{187}Os/^{188}Os$: 0.12470–0.12666) than their protolith (i.e., the Group-2 harzburgites with $^{187}Os/^{188}Os$ ratios from 0.11307 to 0.11651). Hence,
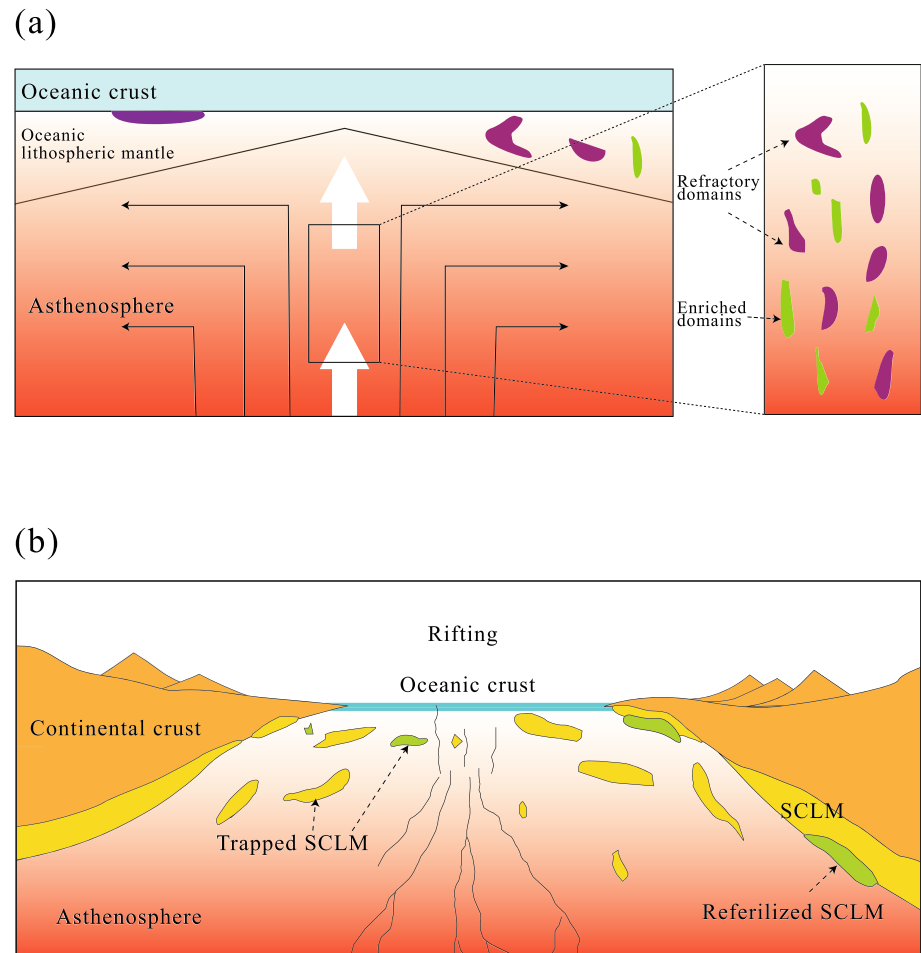
(a)

(b)

Figure 12. Different models of the Shuanggou ophiolitic mantle peridotites. (a) Ancient depleted and refertilized mantles survived from the mantle convection and exhumed during the lithosphere formation (redrawn after Liu et al., 2008) or (2) subcontinental lithospheric mantle (SCLM) incorporation in the upwelling asthenosphere at the continent-ocean transition stage (modified after McCarthy & Müntener, 2015).

magma that derived from or passed through the fertile domains of different ages will inherit the variable isotope signatures and reflect mantle heterogeneity in different scales.

6. Summary

Mantle peridotites in the Shuanggou ophiolite show great heterogeneity. Some of the harzburgites are similar to the typical abyssal peridotites, representing residue of the upwelling asthenosphere. Other harzburgites are more refractory with extremely low $^{187}Os/^{188}Os$ ratios, marking a refractory mantle domain preserved in the oceanic lithosphere, which could be either ancient depleted mantle preserved in the convective mantle or SCLM incorporated in the upwelling asthenosphere. The plagioclase lherzolites in the Shuanggou ophiolite, according to PGE compositions and petrography, are converted from the refractory mantle domains. However, the plagioclase lherzolites have much higher $^{187}Os/^{188}Os$ ratios, which cannot be simply explained by addition of silicate melt. Postrefertilization daughter isotope growth can explain the present $^{187}Os/^{188}Os$ ratios of the lherzolites. REE compositions of the clinopyroxene in the lherzolites reveal that the percolating melt has compositions close to plume-related lavas but different from the Shuanggou diabases and MORB. Thus, we propose the refertilization process took place much earlier than the mantle exhumation beneath the spreading center and was possibly related to the mantle plume activity beneath the Yangtze Block in Protozoic. The generation of fertile and depleted domains that are eventually

sampled at ridges exhibits highly variable isotopic compositions due to postrefertilization isotope growth and greatly contributes to the variability of oceanic basalts.

References

Ackerman, L., Pitcher, L., Strnad, L., Puchtel, I. S., Jelinek, E., Walker, R. J., & Rohovec, J. (2013). Highly siderophile element geochemistry of peridotites and pyroxenites from Horni Bory, Bohemian Massif: Implications for HSE behaviour in subduction-related upper mantle. *Geochimica et Cosmochimica Acta*, *100*, 158–175. https://doi.org/10.1016/j.gca.2012.09.050

Ackerman, L., Walker, R. J., Puchtel, I. S., Pitcher, L., Jelinek, E., & Strnad, L. (2009). Effects of melt percolation on highly siderophile elements and Os isotopes in subcontinental lithospheric mantle: A study of the upper mantle profile beneath Central Europe. *Geochimica et Cosmochimica Acta*, *73*, 2400–2414. https://doi.org/10.1016/j.gca.2009.02.002

Alard, O., Lorand, J.-P., Reisberg, L., Bodinier, J.-L., Dautria, J.-M., & O'Reilly, S. Y. (2011). Volatile-rich metasomatism in Montferrier xenoliths (Southern France): Implications for the abundances of chalcophile and highly siderophile elements in the subcontinental mantle. *Journal of Petrology*, *52*, 2009–2045. https://doi.org/10.1093/petrology/egr038

Alard, O., Luguet, A., Pearson, N. J., Griffin, W. L., Lorand, J.-P., Gannoun, A., et al. (2005). In situ Os isotopes in abyssal peridotites bridge the isotopic gap between MORBs and their source mantle. *Nature*, *436*(7053), 1005–1008. https://doi.org/10.1038/nature03902

Arai, S. (1991). The Circum-Izu Massif peridotites, central Japan, as back-arc mantle fragments of the Izu–Bonin arc system. In T. E. A. Peters (Ed.), *Ophiolite genesis and evolution of the oceanic lithosphere*, (pp. 801–816). Sultanate of Oman: Ministry of Petroleum and Minerals.

Barnes, S. J., Mungall, J. E., & Maier, W. D. (2015). Platinum group elements in mantle melts and mantle samples. *Lithos*, *232*, 395–417. https://doi.org/10.1016/j.lithos.2015.07.007

Barnes, S. J., Naldrett, A. J., & Gorton, M. P. (1985). The origin of the fractionation of platinum-group elements in terrestrial magmas. *Chemical Geology*, *53*, 303–323. https://doi.org/10.1016/0009-2541(85)90076-2

Becker, H., & Dale, C. W. (2016). Re–Pt–Os isotopic and highly siderophile element behavior in oceanic and continental mantle tectonites. *Reviews in Mineralogy and Geochemistry*, *81*(1), 369–440. https://doi.org/10.2138/rmg.2016.81.7

Becker, H., Horan, M. F., Walker, R. J., Gao, S., Lorand, J. P., & Rudnick, R. L. (2006). Highly siderophile element composition of the Earth's primitive upper mantle: Constraints from new data on peridotite massifs and xenoliths. *Geochimica et Cosmochimica Acta*, *70*, 4528–4550. https://doi.org/10.1016/j.gca.2006.06.004

Birck, J. L., Barman, M. R., & Capmas, F. (1997). Re-Os isotopic measurements at the femtomole level in natural samples. *Geostandanrds Newsletter*, *21*, 19–27. https://doi.org/10.1111/j.1751-908x.1997.tb00528.x

Bizimis, M., Griselin, M., Lassiter, J. C., Salters, V. J. M., & Gautam, S. (2007). Ancient recycled mantle lithosphere in the Hawaiian plume: Osmium–hafnium isotopic evidence from peridotite xenoliths. *Earth and Planetary Science Letters*, *257*, 259–273. https://doi.org/10.1016/j.epsl.2007.02.036

Bizimis, M., Salters, V. J., & Bonatti, E. (2000). Trace and REE content of clinopyroxenes from supra-subduction zone peridotites. Implications for melting and enrichment processes in island arcs. *Chemical Geology*, *165*(1-2), 67–85. https://doi.org/10.1016/s0009-2541(99)00164-3

Borghini, G., Rampone, E., Zanetti, A., Class, C., Cipriani, A., Hofmann, A. W., & Goldstein, S. L. (2013). Meter-scale Nd isotopic heterogeneity in pyroxenite-bearing Ligurian peridotites encompasses global-scale upper mantle variability. *Geology*, *41*(10), 1055–1058. https://doi.org/10.1130/g34438.1

Brandon, A. D., Creaser, R. A., Shirey, S. B., & Carlson, R. W. (1996). Osmium recycling in subduction zones. *Science*, *272*(5263), 861–864. https://doi.org/10.1126/science.272.5263.861

Brandon, A. D., Snow, J. E., Walker, R. J., Morgan, J. W., & Mock, T. D. (2000). $^{190}Pt–^{186}Os$ and $^{187}Re–^{187}Os$ systematics of abyssal peridotites. *Earth and Planetary Science Letters*, *177*, 319–335. https://doi.org/10.1016/s0012-821x(00)00044-3

Brenan, J. M., & Andrews, D. (2001). High-temperature stability of laurite and Ru–Os–Ir alloy and their role in PGE fractionation in mafic magmas. *The Canadian Mineralogist*, *39*, 341–360. https://doi.org/10.2113/gscanmin.39.2.341

Buchl, A., Brugmann, G., Batanova, V. G., Munker, C., & Hofmann, A. W. (2002). Melt percolation monitored by Os isotopes and HSE abundances: A case study from the mantle section of the Troodos ophiolite. *Earth and Planetary Science Letters*, *204*, 385–402. https://doi.org/10.1016/s0012-821x(02)00977-9

Bureau of Geology and Mineral Resources of Yunnan Province (BGMRYP) (1990). *Regional geology of Yunnan Province*. Beijing: Geological Publishing House. *(in Chinese)*

Burnham, O., Rogers, N., Pearson, D., Van Calsteren, P., & Hawkesworth, C. (1998). The petrogenesis of the eastern Pyrenean peridotites: An integrated study of their whole-rock geochemistry and Re-Os isotope composition. *Geochimica et Cosmochimica Acta*, *62*, 2293–2310. https://doi.org/10.1016/s0016-7037(98)00092-1

Cannat, M., & Seyler, M. (1995). Transform tectonics, metamorphic plagioclase and amphibolitization in ultramafic rocks of the Vema transform fault (Atlantic Ocean). *Earth and Planetary Science Letters*, *133*, 283–298.

Carlson, R. W., Shirey, S. B., & Schönbächler, M. (2008). Applications of PGE radioisotope systems in geo- and cosmochemistry. *Elements*, *4*, 239–245. https://doi.org/10.2113/gselements.4.4.239

Chen, G., & Xia, B. (2008). Platinum-group elemental geochemistry of mafic and ultramafic rocks from the Xigaze ophiolite, southern Tibet. *Journal of Asian Earth Sciences*, *32*(5-6), 406–422. https://doi.org/10.1016/j.jseaes.2007.11.009

Chesley, J. T., Rudnick, R. L., & Lee, C. T. (1999). Re-Os systematics of mantle xenoliths from the East African Rift: Age, structure, and history of the Tanzanian craton. *Geochimica et Cosmochimica Acta*, *63*(7-8), 1203–1217. https://doi.org/10.1016/s0016-7037(99)00004-6

Chu, Z. Y., Wu, F. Y., Walker, R. J., Rudnick, R. L., Pitcher, L., Puchtel, I. S., et al. (2009). Temporal evolution of the lithospheric mantle beneath the eastern North China Craton. *Journal of Petrology*, *50*, 1857–1898. https://doi.org/10.1093/petrology/egp055

Cipriani, A., Brueckner, H. K., Bonatti, E., & Brunelli, D. (2004). Oceanic crust generated by elusive parents: Sr and Nd isotopes in basalt-peridotite pairs from the Mid-Atlantic Ridge. *Geology*, *32*, 657–660. https://doi.org/10.1130/g20560.1

Cohen, A. S., & Waters, F. G. (1996). Separation of osmium from geological materials by solvent extraction for analysis by thermal ionisation mass spectrometry. *Analytica Chimica Acta*, *332*(2-3), 269–275. https://doi.org/10.1016/0003-2670(96)00226-7

Coleman, R. G. (1967). Low-temperature reaction zones and alpine ultramafic rocks of California, Oregon, and Washington. *U.S. Geological Survey Bulletin*, *1247*, 49. https://doi.org/10.3133/b1247

Coltorti, M., Bonadiman, C., O'Reilly, S. Y., Griffin, W. L., & Pearson, N. J. (2010). Buoyant ancient continental mantle embedded in oceanic lithosphere (Sal Island, Cape Verde Archipelago). *Lithos*, *120*(1), 223–233. https://doi.org/10.1016/j.lithos.2009.11.005

Dai, J. G., Wang, C. S., Hébert, R., Santosh, M., Li, Y. L., & Xu, J. Y. (2011). Petrology and geochemistry of peridotites in the Zhongba ophiolite, Yarlung Zangbo Suture Zone: Implications for the Early Cretaceous intra-oceanic subduction zone within the Neo-Tethys. *Chemical Geology*, *288*(3-4), 133–148. https://doi.org/10.1016/j.chemgeo.2011.07.011

Day, J. M., Walker, R. J., & Warren, J. M. (2017). ^{186}Os–^{187}Os and highly siderophile element abundance systematics of the mantle revealed by abyssal peridotites and Os-rich alloys. *Geochimica et Cosmochimica Acta*, *200*, 232–254. https://doi.org/10.1016/j.gca.2016.12.013

Deng, J., Wang, Q., Li, G., Li, C., & Wang, C. (2014). Tethys tectonic evolution and its bearing on the distribution of important mineral deposits in the Sanjiang region, SW China. *Gondwana Research*, *26*(2), 419–437. https://doi.org/10.1016/j.gr.2013.08.002

Dick, H. J. B. (1989). Abyssal peridotites, very slow spreading ridges and ocean ridge magmatism. *Geological Society, London, Special Publications*, *42*(1), 71–105. https://doi.org/10.1144/gsl.sp.1989.042.01.06

Elthon, D. (1992). Chemical trends in abyssal peridotites: Refertilization of depleted suboceanic mantle. *Journal of Geophysical Research, Solid Earth*, *97*(B6), 9015–9025. https://doi.org/10.1029/92jb00723

Evans, B. W., Hattori, K., & Baronnet, A. (2013). Serpentinite: What, why, where? *Elements*, *9*(2), 99–106. https://doi.org/10.2113/gselements.9.2.99

Fan, H. P., Zhu, W. G., Li, Z. X., Zhong, H., Bai, Z. J., He, D. F., et al. (2013). Ca. 1.5 Ga mafic magmatism in South China during the break-up of the supercontinent Nuna/Columbia: The Zhuqing Fe–Ti–V oxide ore-bearing mafic intrusions in western Yangtze Block. *Lithos*, *168*, 85–98. https://doi.org/10.1016/j.lithos.2013.02.004

Fischer-Gödde, M., Becker, H., & Wombacher, F. (2010). Rhodium, gold and other highly siderophile element abundances in chondritic meteorites. *Geochimica et Cosmochimica Acta*, *74*(1), 356–379. https://doi.org/10.1016/j.gca.2009.09.024

Fischer-Gödde, M., Becker, H., & Wombacher, F. (2011). Rhodium, gold and other highly siderophile elements in orogenic peridotites and peridotite xenoliths. *Chemical Geology*, *280*(3), 365–383. https://doi.org/10.1016/j.chemgeo.2010.11.024

Foley, S. F. (2008). Rejuvenation and erosion of the cratonic lithosphere. *Nature Geoscience*, *1*(8), 503. https://doi.org/10.1038/ngeo261

Fonseca, R. O., Laurenz, V., Mallmann, G., Luguet, A., Hoehne, N., & Jochum, K. P. (2012). New constraints on the genesis and long-term stability of Os-rich alloys in the Earth's mantle. *Geochimica et Cosmochimica Acta*, *87*, 227–242. https://doi.org/10.1016/j.gca.2012.04.002

Fonseca, R. O., Mallmann, G., O'Neill, H. S. C., Campbell, I. H., & Laurenz, V. (2011). Solubility of Os and Ir in sulfide melt: Implications for Re/Os fractionation during mantle melting. *Earth and Planetary Science Letters*, *311*(3-4), 339–350. https://doi.org/10.1016/j.epsl.2011.09.035

Hamlyn, P. R., & Bonatti, E. (1980). Petrology of mantle-derived ultramafics from the Owen Fracture Zone, northwest Indian Ocean: Implications for the nature of the oceanic upper mantle. *Earth and Planetary Science Letters*, *48*(1), 65–79. https://doi.org/10.1016/0012-821x(80)90171-5

Harvey, J., Dale, C. W., Gannoun, A., & Burton, K. W. (2011). Osmium mass balance in peridotite and the effects of mantle-derived sulphides on basalt petrogenesis. *Geochimica et Cosmochimica Acta*, *75*(19), 5574–5596. https://doi.org/10.1016/j.gca.2011.07.001

Harvey, J., Gannoun, A., Burton, K. W., Rogers, N. W., Alard, O., & Parkinson, I. J. (2006). Ancient melt extraction from the oceanic upper mantle revealed by Re–Os isotopes in abyssal peridotites from the Mid-Atlantic ridge. *Earth and Planetary Science Letters*, *244*(3), 606–621. https://doi.org/10.1016/j.epsl.2006.02.031

Harvey, J., Gannoun, A., Burton, K. W., Schiano, P., Rogers, N. W., & Alard, O. (2010). Unravelling the effects of melt depletion and secondary infiltration on mantle Re–Os isotopes beneath the French Massif Central. *Geochimica et Cosmochimica Acta*, *74*(1), 293–320. https://doi.org/10.1016/j.gca.2009.09.031

Hauri, E. H., & Hart, S. R. (1997). Rhenium abundances and systematics in oceanic basalts. *Chemical Geology*, *139*(1), 185–205. https://doi.org/10.1016/s0009-2541(97)00035-1

Hirschmann, M. M., & Stolper, E. M. (1996). A possible role for garnet pyroxenite in the origin of the "garnet signature" in MORB. *Contributions to Mineralogy and Petrology*, *124*(2), 185–208. https://doi.org/10.1007/s004100050184

Hu, W. J., Zhong, H., Zhu, W. G., & He, X. H. (2014). Elemental and Sr-Nd isotopic geochemistry of the basalts and microgabbros in the Shuanggou ophiolite, SW China: Implication for the evolution of the Palaeotethys Ocean. *Geological Magazine*, *152*, 210–224. https://doi.org/10.1017/s0016756814000259

Hu, Z. C., Gao, S., Liu, Y. S., Hu, S. H., Chen, H. H., & Yuan, H. L. (2008). Signal enhancement in laser ablation ICP-MS by addition of nitrogen in the central channel gas. *Journal of Analytical Atomic Spectrometry*, *23*, 1093–1101. https://doi.org/10.1039/b804760j

Hyndman, R. D., & Peacock, S. M. (2003). Serpentinization of the forearc mantle. *Earth and Planetary Science Letters*, *212*(3-4), 417–432. https://doi.org/10.1016/s0012-821x(03)00263-2

Ionov, D. A., Carlson, R. W., Doucet, L. S., Golovin, A. V., & Oleinikov, O. B. (2015). The age and history of the lithospheric mantle of the Siberian craton: Re–Os and PGE study of peridotite xenoliths from the Obnazhennaya kimberlite. *Earth and Planetary Science Letters*, *428*, 108–119. https://doi.org/10.1016/j.epsl.2015.07.007

Ionov, D. A., Doucet, L. S., Carlson, R. W., Golovin, A. V., & Korsakov, A. V. (2015). Post-Archean formation of the lithospheric mantle in the central Siberian craton: Re–Os and PGE study of peridotite xenoliths from the Udachnaya kimberlite. *Geochimica et Cosmochimica Acta*, *165*, 466–483. https://doi.org/10.1016/j.gca.2015.06.035

Ionov, D. A., Prikhodko, V. S., Bodinier, J. L., Sobolev, A. V., & Weis, D. (2005). Lithospheric mantle beneath the south-eastern Siberian craton: Petrology of peridotite xenoliths in basalts from the Tokinsky Stanovik. *Contributions to Mineralogy and Petrology*, *149*(6), 647–665. https://doi.org/10.1007/s00410-005-0672-9

Ionov, D. A., Shirey, S. B., Weis, D., & Brügmann, G. (2006). Os–Hf–Sr–Nd isotope and PGE systematics of spinel peridotite xenoliths from Tok, SE Siberian craton: Effects of pervasive metasomatism in shallow refractory mantle. *Earth and Planetary Science Letters*, *241*(1-2), 47–64. https://doi.org/10.1016/j.epsl.2005.10.038

Jean, M. M., Shervais, J. W., Choi, S. H., & Mukasa, S. B. (2010). Melt extraction and melt refertilization in mantle peridotite of the Coast Range ophiolite: An LA–ICP–MS study. *Contributions to Mineralogy and Petrology*, *159*(1), 113. https://doi.org/10.1007/s00410-009-0419-0

Jian, P., Liu, D., Kröner, A., Zhang, Q., Wang, Y., Sun, X., & Zhang, W. (2009a). Devonian to Permian plate tectonic cycle of the Paleo-Tethys Orogen in southwest China (I): Geochemistry of ophiolites, arc/back-arc assemblages and within-plate igneous rocks. *Lithos*, *113*(3-4), 748–766. https://doi.org/10.1016/j.lithos.2009.04.004

Jian, P., Liu, D., Kröner, A., Zhang, Q., Wang, Y., Sun, X., & Zhang, W. (2009b). Devonian to Permian plate tectonic cycle of the Paleo-Tethys Orogen in southwest China (II): Insights from zircon ages of ophiolites, arc/back-arc assemblages and within-plate igneous rocks and generation of the Emeishan CFB province. *Lithos*, *113*(3-4), 767–784. https://doi.org/10.1016/j.lithos.2009.04.006

Kamenetsky, V. S., Chung, S. L., Kamenetsky, M. B., & Kuzmin, D. V. (2012). Picrites from the Emeishan Large Igneous Province, SW China: A compositional continuum in primitive magmas and their respective mantle sources. *Journal of Petrology*, *53*(10), 2095–2113. https://doi.org/10.1093/petrology/egs045

Kelemen, P. B., Hanghøj, K., & Greene, A. R. (2003). One view of the geochemistry of subduction-related magmatic arcs, with an emphasis on primitive andesite and lower crust. *Treatise on Geochemistry*, *3*, 593–659. https://doi.org/10.1016/B0-08-043751-6/03035-8

Kepezhinskas, P., Defant, M. J., & Widom, E. (2002). Abundance and distribution of PGE and Au in the island-arc mantle: Implications for sub-arc metasomatism. *Lithos*, *60*(3-4), 113–128. https://doi.org/10.1016/s0024-4937(01)00073-1

Kogiso, T., Hirschmann, M. M., & Pertermann, M. (2004). High-pressure partial melting of mafic lithologies in the mantle. *Journal of Petrology*, *45*(12), 2407–2422. https://doi.org/10.1093/petrology/egh057

Lai, C. K., Meffre, S., Crawford, A. J., Zaw, K., Xue, C. D., & Halpin, J. A. (2014). The western Ailaoshan volcanic belts and their SE Asia connection: A new tectonic model for the Eastern Indochina Block. *Gondwana Research*, *26*(1), 52–74. https://doi.org/10.1016/j.gr.2013.03.003

Lassiter, J. C., Byerly, B. L., Snow, J. E., & Hellebrand, E. (2014). Constraints from Os-isotope variations on the origin of Lena Trough abyssal peridotites and implications for the composition and evolution of the depleted upper mantle. *Earth and Planetary Science Letters*, *403*, 178–187. https://doi.org/10.1016/j.epsl.2014.05.033

Le Roux, V., Bodinier, J. L., Tommasi, A., Alard, O., Dautria, J. M., Vauchez, A., & Riches, A. J. V. (2007). The Lherz spinel lherzolite: Refertilized rather than pristine mantle. *Earth and Planetary Science Letters*, *259*(3), 599–612. https://doi.org/10.1016/j.epsl.2007.05.026

Le Roux, V., Dick, H. J. B., & Shimizu, N. (2014). Tracking flux melting and melt percolation in supra-subduction peridotites (Josephine ophiolite, USA). *Contributions to Mineralogy and Petrology*, *168*(4), 1064. https://doi.org/10.1007/s00410-014-1064-9

Le Roux, V., & Liang, Y. (2019). Ophiolitic pyroxenites record boninite percolation in subduction zone mantle. *Minerals*, *9*(9), 565. https://doi.org/10.3390/min9090565

Le Roux, V., Nielsen, S. G., Sun, C., & Yao, L. (2016). Dating layered websterite formation in the lithospheric mantle. *Earth and Planetary Science Letters*, *454*, 103–112. https://doi.org/10.1016/j.epsl.2016.08.036

Lee, C. T. A., Luffi, P., & Chin, E. J. (2011). Building and destroying continental mantle. *Annual Review of Earth and Planetary Sciences*, *39*, 59–90. https://doi.org/10.1146/annurev-earth-040610-133505

Leloup, P. H., Lacassin, R., Tapponnier, P., Schärer, U., Zhong, D., Liu, X., et al. (1995). The Ailao Shan-Red River shear zone (Yunnan, China), Tertiary transform boundary of Indochina. *Tectonophysics*, *251*(1-4), 3–84. https://doi.org/10.1016/0040-1951(95)00070-4

Liu, C. Z., Snow, J. E., Brügmann, G., Hellebrand, E., & Hofmann, A. W. (2009). Non-chondritic HSE budget in Earth's upper mantle evidenced by abyssal peridotites from Gakkel ridge (Arctic Ocean). *Earth and Planetary Science Letters*, *283*(1-4), 122–132. https://doi.org/10.1016/j.epsl.2009.04.002

Liu, C. Z., Snow, J. E., Hellebrand, E., Brügmann, G., Von Der Handt, A., Büchl, A., & Hofmann, A. W. (2008). Ancient, highly hetero-geneous mantle beneath Gakkel ridge, Arctic Ocean. *Nature*, *452*(7185), 311–316. https://doi.org/10.1038/nature06688

Liu, C. Z., Wu, F. Y., Wilde, S. A., Yu, L. J., & Li, J. L. (2010). Anorthitic plagioclase and pargasitic amphibole in mantle peridotites from the Yungbwa ophiolite (southwestern Tibetan Plateau) formed by hydrous melt metasomatism. *Lithos*, *114*(3-4), 413–422. https://doi.org/10.1016/j.lithos.2009.10.008

Liu, T., Wu, F. Y., Liu, C. Z., Zhang, C., Ji, W. B., & Xu, Y. (2019). Reconsideration of Neo-Tethys evolution constrained from the nature of the Dazhuqu ophiolitic mantle, southern Tibet. *Contributions to Mineralogy and Petrology*, *174*(3), 23. https://doi.org/10.1007/s00410-019-1557-7

Liu, Y., Hu, Z., Gao, S., Günther, D., Xu, J., Gao, C., & Chen, H. (2008). In situ analysis of major and trace elements of anhydrous minerals by LA-ICP-MS without applying an internal standard. *Chemical Geology*, *257*(1-2), 34–43. https://doi.org/10.1016/j.chemgeo.2008.08.004

Lorand, J. P., Alard, O., & Godard, M. (2009). Platinum-group element signature of the primitive mantle rejuvenated by melt-rock reac-tions: Evidence from Sumail peridotites (Oman Ophiolite). *Terra Nova*, *21*(1), 35–40. https://doi.org/10.1111/j.1365-3121.2008.00850.x

Lorand, J. P., Luguet, A., & Alard, O. (2008). Platinum-group elements: A new set of key tracers for the Earth's interior. *Elements*, *4*(4), 247–252. https://doi.org/10.2113/gselements.4.4.247

Lorand, J. P., Luguet, A., & Alard, O. (2013). Platinum-group element systematics and petrogenetic processing of the continental upper mantle: A review. *Lithos*, *164*, 2–21. https://doi.org/10.1016/j.lithos.2012.08.017

Lu, G., Wang, W., Ernst, R. E., Söderlund, U., Lan, Z., Huang, S., & Xue, E. (2019). Petrogenesis of Paleo-Mesoproterozoic mafic rocks in the southwestern Yangtze Block of South China: Implications for tectonic evolution and paleogeographic reconstruction. *Precambrian Research*, *322*, 66–84. https://doi.org/10.1016/j.precamres.2018.12.019

Luguet, A., Shirey, S. B., Lorand, J. P., Horan, M. F., & Carlson, R. W. (2007). Residual platinum-group minerals from highly depleted harzburgites of the Lherz massif (France) and their role in HSE fractionation of the mantle. *Geochimica et Cosmochimica Acta*, *71*(12), 3082–3097. https://doi.org/10.1016/j.gca.2007.04.011

Mallmann, G., & O'Neill, H. S. C. (2007). The effect of oxygen fugacity on the partitioning of Re between crystals and silicate melt during mantle melting. *Geochimica et Cosmochimica Acta*, *71*(11), 2837–2857. https://doi.org/10.1016/j.gca.2007.03.028

Marchesi, C., Dale, C. W., Garrido, C. J., Pearson, D. G., Bosch, D., Bodinier, J. L., et al. (2014). Fractionation of highly siderophile elements in refertilized mantle: Implications for the Os isotope composition of basalts. *Earth and Planetary Science Letters*, *400*, 33–44. https://doi.org/10.1016/j.epsl.2014.05.025

McCarthy, A., & Müntener, O. (2015). Ancient depletion and mantle heterogeneity: Revisiting the Permian-Jurassic paradox of Alpine peridotites. *Geology*, *43*(3), 255–258. https://doi.org/10.1130/g36340.1

Meisel, T., Walker, R. J., Irving, A. J., & Lorand, J. P. (2001). Osmium isotopic compositions of mantle xenoliths: A global perspective. *Geochimica et Cosmochimica Acta*, *65*(8), 1311–1323. https://doi.org/10.1016/s0016-7037(00)00566-4

Meisel, T., Walker, R. J., & Morgan, J. W. (1996). The osmium isotopic composition of the Earth's primitive upper mantle. *Nature*, *383*, 517–520. https://doi.org/10.1038/383517a0

Metcalfe, I. (1996). Gondwanaland dispersion, Asian accretion and evolution of eastern Tethys. *Australian Journal of Earth Sciences*, *43*(6), 605–623. https://doi.org/10.1080/08120099608728282

Metcalfe, I. (2006). Palaeozoic and Mesozoic tectonic evolution and palaeogeography of East Asian crustal fragments: The Korean Peninsula in context. *Gondwana Research*, *9*(1-2), 24–46. https://doi.org/10.1016/j.gr.2005.04.002

Mével, C. (2003). Serpentinization of abyssal peridotites at mid-ocean ridges. *Comptes Rendus Geoscience*, *335*(10-11), 825–852. https://doi.org/10.1016/j.crte.2003.08.006

Mo, X. X., Shen, S. Y., Zhu, Q. W., Xu, T., Wei, Q., Tan, J., et al. (1998). *Volcanics-ophiolite and mineralization of middle-southern part in Sanjiang area of southwestern China*. Beijing: Geological Publishing House. (in Chinese)

Montanini, A., Tribuzio, R., & Vernia, L. (2008). Petrogenesis of basalts and gabbros from an ancient continent–ocean transition (external Liguride ophiolites, northern Italy). *Lithos*, *101*(3-4), 453–479. https://doi.org/10.1016/j.lithos.2007.09.007

Müntener, O., Manatschal, G., Desmurs, L., & Pettke, T. (2010). Plagioclase peridotites in ocean–continent transitions: Refertilized mantle domains generated by melt stagnation in the shallow mantle lithosphere. *Journal of Petrology*, *51*(1-2), 255–294. https://doi.org/10.1093/petrology/egp087

Müntener, O., Pettke, T., Desmurs, L., Meier, M., & Schaltegger, U. (2004). Refertilization of mantle peridotite in embryonic ocean basins: Trace element and Nd isotopic evidence and implications for crust–mantle relationships. *Earth and Planetary Science Letters*, *221*(1-4), 293–308. https://doi.org/10.1016/s0012-821x(04)00073-1

Nicolas, A., & Dupuy, C. (1984). Origin of ophiolitic and oceanic lherzolites. *Tectonophysics*, *110*(3-4), 177–187. https://doi.org/10.1016/0040-1951(84)90259-2

O'Driscoll, B., Day, J. M., Walker, R. J., Daly, J. S., McDonough, W. F., & Piccoli, P. M. (2012). Chemical heterogeneity in the upper mantle recorded by peridotites and chromitites from the Shetland Ophiolite Complex, Scotland. *Earth and Planetary Science Letters*, *333*, 226–237. https://doi.org/10.1016/j.epsl.2012.03.035

O'driscoll, B., Walker, R. J., Day, J. M., Ash, R. D., & Daly, J. S. (2015). Generations of melt extraction, melt–rock interaction and high-temperature metasomatism preserved in peridotites of the ~497 Ma Leka Ophiolite Complex, Norway. *Journal of Petrology*, *56*(9), 1797–1828. https://doi.org/10.1093/petrology/egv055

O'Reilly, S. Y., Zhang, M., Griffin, W. L., Begg, G., & Hronsky, J. (2009). Ultradeep continental roots and their oceanic remnants: A solution to the geochemical "mantle reservoir" problem? *Lithos*, *112*, 1043–1054. https://doi.org/10.1016/j.lithos.2009.04.028

Pamić, J., Tomljenović, B., & Balen, D. (2002). Geodynamic and petrogenetic evolution of Alpine ophiolites from the central and NW Dinarides: An overview. *Lithos*, *65*(1-2), 113–142. https://doi.org/10.1016/s0024-4937(02)00162-7

Parkinson, I. J., & Pearce, J. A. (1998). Peridotites from the Izu–Bonin–Mariana forearc (ODP Leg 125): Evidence for mantle melting and melt–mantle interaction in a supra-subduction zone setting. *Journal of Petrology*, *39*(9), 1577–1618. https://doi.org/10.1093/petrology/39.9.1577

Pearson, D. G., Irvine, G. J., Ionov, D. A., Boyd, F. R., & Dreibus, G. E. (2004). Re–Os isotope systematics and platinum group element fractionation during mantle melt extraction: A study of massif and xenolith peridotite suites. *Chemical Geology*, *208*(1-4), 29–59. https://doi.org/10.1016/j.chemgeo.2004.04.005

Pernet-Fisher, J. F., Howarth, G. H., Pearson, D. G., Woodland, S., Barry, P. H., Pokhilenko, N. P., et al. (2015). Plume impingement on the Siberian SCLM: Evidence from Re–Os isotope systematics. *Lithos*, *218*, 141–154. https://doi.org/10.1016/j.lithos.2015.01.010

Piccardo, G. B., Müntener, O., & Zanetti, A. (2004). Alpine–Apennine ophiolitic peridotites: New concepts on their composition and evolution. *Ofioliti*, *29*(1), 63–74.

Pirnia, T., Saccani, E., & Arai, S. (2018). Spinel and plagioclase peridotites of the Nain ophiolite (Central Iran): Evidence for the incipient stage of oceanic basin formation. *Lithos*, *310*, 1–19. https://doi.org/10.1016/j.lithos.2018.04.001

Qi, L., Gao, J., Huang, X., Hu, J., Zhou, M. F., & Zhong, H. (2011). An improved digestion technique for determination of platinum group elements in geological samples. *Journal of Analytical Atomic Spectrometry*, *26*(9), 1900–1904. https://doi.org/10.1039/c1ja10114e

Qi, L., Hu, J., & Gregoire, D. C. (2000). Determination of trace elements in granites by inductively coupled plasma mass spectrometry. *Talanta*, *51*(3), 507–513. https://doi.org/10.1016/s0039-9140(99)00318-5

Qi, L., Zhou, M. F., & Wang, C. Y. (2004). Determination of low concentrations of platinum group elements in geological samples by ID-ICP-MS. *Journal of Analytical Atomic Spectrometry*, *19*(10), 1335–1339. https://doi.org/10.1039/B400742E

Rampone, E., & Hofmann, A. W. (2012). A global overview of isotopic heterogeneities in the oceanic mantle. *Lithos*, *148*, 247–261. https://doi.org/10.1016/j.lithos.2012.06.018

Rampone, E., Piccardo, G. B., Vannucci, R., & Bottazzi, P. (1997). Chemistry and origin of trapped melts in ophioiitic peridotites. *Geochimica et Cosmochimica Acta*, *61*(21), 4557–4569. https://doi.org/10.1016/s0016-7037(97)00260-3

Rampone, E., Piccardo, G. B., Vannucci, R., Bottazzi, P., & Zanetti, A. (1994). Melt impregnation in ophiolitic peridotite: An ion microprobe study of clinopyroxene and plagioclase. *Mineralogical Magazine*, *58*(2), 756–757. https://doi.org/10.1180/minmag.1994.58a.2.130

Rampone, E., Vissers, R. L. M., Poggio, M., Scambelluri, M., & Zanetti, A. (2009). Melt migration and intrusion during exhumation of the Alboran lithosphere: The Tallante mantle xenolith record (Betic Cordillera, SE Spain). *Journal of Petrology*, *51*(1-2), 295–325. https://doi.org/10.1093/petrology/egp061

Rehkaemper, M., Halliday, A. N., Fitton, J. G., Lee, D. C., Wieneke, M., & Arndt, N. T. (1999). Ir, Ru, Pt, and Pd in basalts and komatiites: New constraints for the geochemical behavior of the platinum-group elements in the mantle. *Geochimica et Cosmochimica Acta*, *63*(22), 3915–3934. https://doi.org/10.1016/s0016-7037(99)00219-7

Reisberg, L., & Lorand, J. P. (1995). Longevity of sub-continental mantle lithosphere from osmium isotope systematics in orogenic peridotite massifs. *Nature*, *376*(6536), 159–162. https://doi.org/10.1038/376159a0

Reisberg, L., Rouxel, O., Ludden, J., Staudigel, H., & Zimmermann, C. (2008). Re–Os results from ODP Site 801: Evidence for extensive Re uptake during alteration of oceanic crust. *Chemical Geology*, *248*(3), 256–271. https://doi.org/10.1016/j.chemgeo.2007.07.013

Rudnick, R. L., & Walker, R. J. (2009). Interpreting ages from Re–Os isotopes in peridotites. *Lithos*, *112*, 1083–1095. https://doi.org/10.1016/j.lithos.2009.04.042

Saal, A. E., Takazawa, E., Frey, F. A., Shimizu, N., & Hart, S. R. (2001). Re–Os isotopes in the Horoman peridotite: Evidence for refertilization? *Journal of Petrology*, *42*(1), 25–37. https://doi.org/10.1093/petrology/42.1.25

Saha, A., Basu, A. R., Jacobsen, S. B., Poreda, R. J., Yin, Q. Z., & Yogodzinski, G. M. (2005). Slab devolatilization and Os and Pb mobility in the mantle wedge of the Kamchatka arc. *Earth and Planetary Science Letters*, *236*(1-2), 182–194. https://doi.org/10.1016/j.epsl.2005.05.018

Schaltegger, U., Desmurs, L., Manatschal, G., Müntener, O., Meier, M., Frank, M., & Bernoulli, D. (2002). The transition from rifting to seafloor spreading within a magma-poor rifted margin: Field and isotopic constraints. *Terra Nova*, *14*(3), 156–162. https://doi.org/10.1046/j.1365-3121.2002.00406.x

Schulte, R. F., Schilling, M., Anma, R., Farquhar, J., Horan, M. F., Komiya, T., et al. (2009). Chemical and chronologic complexity in the convecting upper mantle: Evidence from the Taitao ophiolite, southern Chile. *Geochimica et Cosmochimica Acta*, *73*(19), 5793–5819. https://doi.org/10.1016/j.gca.2009.06.015

Searle, M. P., Yeh, M. W., Lin, T. H., & Chung, S. L. (2010). Structural constraints on the timing of left-lateral shear along the Red River shear zone in the Ailao Shan and Diancang Shan Ranges, Yunnan, SW China. *Geosphere*, *6*(4), 316–338. https://doi.org/10.1130/ges00580.1

Sempéré, J. C., Lin, J., Brown, H. S., Schouten, H., & Purdy, G. M. (1993). Segmentation and morphotectonic variations along a slow-spreading center: The Mid-Atlantic Ridge (24°00′N–30°40′N). *Marine Geophysical Researches*, *15*(3), 153–200. https://doi.org/10.1007/bf01204232

Smoliar, M. I., Walker, R. J., & Morgan, J. W. (1996). Re-Os ages of group IIA, IIIA, IVA, and IVB iron meteorites. *Science*, *271*(5252), 1099–1102. https://doi.org/10.1126/science.271.5252.1099

Snow, J. E., & Reisberg, L. (1995). Os isotopic systematics of the MORB mantle: Results from altered abyssal peridotites. *Earth and Planetary Science Letters*, *133*(3-4), 411–421. https://doi.org/10.1016/0012-821x(95)00099-x

Stracke, A. (2008). Chemical geodynamics: Tracking mantle depletion. *Nature Geoscience*, *1*(4), 215. https://doi.org/10.1038/ngeo163

Sun, C., & Liang, Y. (2012). Distribution of REE between clinopyroxene and basaltic melt along a mantle adiabat: Effects of major element composition, water, and temperature. *Contributions to Mineralogy and Petrology*, *163*(5), 807–823. https://doi.org/10.1007/s00410-011-0700-x

Sun, J., Liu, C. Z., Kostrovisky, S. I., Wu, F. Y., Yang, J. H., Chu, Z. Y., et al. (2017). Composition of the lithospheric mantle in the northern part of Siberian craton: Constraints from peridotites in the Obnazhennaya kimberlite. *Lithos*, *294*, 383–396. https://doi.org/10.1016/j.lithos.2017.10.010

Sun, S. S., & McDonough, W. S. (1989). Chemical and isotopic systematics of oceanic basalts: Implications for mantle composition and processes. *Geological Society, London, Special Publications*, *42*(1), 313–345. https://doi.org/10.1144/gsl.sp.1989.042.01.19

Takazawa, E., Frey, F. A., Shimizu, N., & Obata, M. (2000). Whole rock compositional variations in an upper mantle peridotite (Horoman, Hokkaido, Japan): Are they consistent with a partial melting process? *Geochimica et Cosmochimica Acta*, *64*(4), 695–716. https://doi.org/10.1016/s0016-7037(99)00346-4

Tang, Y. J., Zhang, H. F., Ying, J. F., & Su, B. X. (2013). Widespread refertilization of cratonic and circum-cratonic lithospheric mantle. *Earth-Science Reviews*, *118*, 45–68. https://doi.org/10.1016/j.earscirev.2013.01.004

Walker, R. J., Carlson, R. W., Shirey, S. B., & Boyd, F. R. (1989). Os, Sr, Nd, and Pb isotope systematics of southern African peridotite xenoliths: Implications for the chemical evolution of subcontinental mantle. *Geochimica et Cosmochimica Acta*, *53*(7), 1583–1595. https://doi.org/10.1016/0016-7037(89)90240-8

Wang, X., Metcalfe, I., Jian, P., He, L., & Wang, C. (2000). The Jinshajiang–Ailaoshan suture zone, China: Tectonostratigraphy, age and evolution. *Journal of Asian Earth Sciences*, *18*(6), 675–690. https://doi.org/10.1016/s1367-9120(00)00039-0

Wang, Y., Fan, W., Zhang, Y., Peng, T., Chen, X., & Xu, Y. (2006). Kinematics and 40Ar/39Ar geochronology of the Gaoligong and Chongshan shear systems, western Yunnan, China: Implications for early Oligocene tectonic extrusion of SE Asia. *Tectonophysics*, *418*(3-4), 235–254. https://doi.org/10.1016/j.tecto.2006.02.005

Wang, Y., Li, X., Duan, L. L., Huang, Z. X., & Chui, C. (2000). *Geotectonics and metallogeny in South Nujiang-Lanchang-Jinsha Rivers area*. (in Chinese).

Wang, Z., Becker, H., & Gawronski, T. (2013). Partial re-equilibration of highly siderophile elements and the chalcogens in the mantle: A case study on the Baldissero and Balmuccia peridotite massifs (Ivrea Zone, Italian Alps). *Geochimica et Cosmochimica Acta*, *108*, 21–44. https://doi.org/10.1016/j.gca.2013.01.021

Warren, J. M. (2016). Global variations in abyssal peridotite compositions. *Lithos*, *248*, 193–219. https://doi.org/10.1016/j.lithos.2015.12.023

Warren, J. M., Shimizu, N., Sakaguchi, C., Dick, H. J., & Nakamura, E. (2009). An assessment of upper mantle heterogeneity based on abyssal peridotite isotopic compositions. *Journal of Geophysical Research, Solid Earth*, *114*(B12). https://doi.org/10.1029/2008jb006186

Widom, E., Kepezhinskas, P., & Defant, M. (2003). The nature of metasomatism in the sub-arc mantle wedge: Evidence from Re–Os isotopes in Kamchatka peridotite xenoliths. *Chemical Geology*, *196*(1-4), 283–306. https://doi.org/10.1016/s0009-2541(02)00417-5

Yan, Q., Wang, Z., Liu, S., Li, Q., Zhang, H., Wang, T., et al. (2005). Opening of the Tethys in southwest China and its significance to the breakup of East Gondwanaland in late Paleozoic: Evidence from SHRIMP U-Pb zircon analyses for the Garzê ophiolite block. *Chinese Science Bulletin*, *50*(3), 256–264. https://doi.org/10.1007/bf02897536

Yaxley, G. M. (2000). Experimental study of the phase and melting relations of homogeneous basalt+ peridotite mixtures and implications for the petrogenesis of flood basalts. *Contributions to Mineralogy and Petrology*, *139*(3), 326–338. https://doi.org/10.1007/s004100000134

Zhang, Q., Zhou, D., & Li, X. (1995). Characteristics and genesis of Shuanggou ophiolites, Yunnan Province, China. *Acta Petrol Sin (in Chinese)*, *11*, 190–202.

Zhao, G., Cawood, P. A., Wilde, S. A., & Sun, M. (2002). Review of global 2.1–1.8 Ga orogens: Implications for a pre-Rodinia supercontinent. *Earth-Science Reviews*, *59*(1-4), 125–162. https://doi.org/10.1016/s0012-8252(02)00073-9

Zhao, X. F., Zhou, M. F., Li, J. W., Sun, M., Gao, J. F., Sun, W. H., & Yang, J. H. (2010). Late Paleoproterozoic to early Mesoproterozoic Dongchuan Group in Yunnan, SW China: Implications for tectonic evolution of the Yangtze Block. *Precambrian Research*, *182*(1-2), 57–69. https://doi.org/10.1016/j.precamres.2010.06.021

Zheng, J. P., Lee, C. T., Lu, J. G., Zhao, J. H., Wu, Y. B., Xia, B., et al. (2015). Refertilization-driven destabilization of subcontinental mantle and the importance of initial lithospheric thickness for the fate of continents. *Earth and Planetary Science Letters*, *409*, 225–231. https://doi.org/10.1016/j.epsl.2014.10.042

Zhong, D. L. (1998). *Paleo-Tethyan orogenic belt in western Yunnan and Sichuan*. Beijing: Science Press. (in Chinese)

Zhou, D. J., Zhang, Q., Li, X. Y., Chen, Y., Huang, Z. X., Han, S., et al. (1995). Geochemistry of initial melting in Shuanggou mantle rock, Yunnan Province, China. *Acta Petrol Sin (in Chinese)*, *11*, 203–211.

Zi, J. W., Cawood, P. A., Fan, W. M., Wang, Y. J., & Tohver, E. (2012). Contrasting rift and subduction-related plagiogranites in the Jinshajiang ophiolitic mélange, southwest China, and implications for the Paleo-Tethys. *Tectonics*, *31*, TC2012. https://doi.org/10.1029/2011tc002937